論文 / 著書情報
Article / Book Information

Title	JENDL-5 benchmark test for shielding applications
Authors	Chikara Konno, Masayuki Ohta, Saerom Kwon, Seiki Ohnishi, Naoki Yamano, Satoshi Sato
Citation	Journal of Nuclear Science and Technology, Volume 60, Issue 9, Page 1046-1069
Pub. date	2023, 2
DOI	https://doi.org/10.1080/00223131.2022.2164372
Creative Commons	Information is in the article.

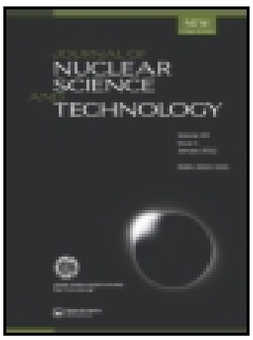

Journal of Nuclear Science and Technology

ISSN: (Print) (Online) Journal homepage: https://www.tandfonline.com/loi/tnst20

JENDL-5 benchmark test for shielding applications

Chikara Konno, Masayuki Ohta, Saerom Kwon, Seiki Ohnishi, Naoki Yamano & Satoshi Sato

To cite this article: Chikara Konno, Masayuki Ohta, Saerom Kwon, Seiki Ohnishi, Naoki Yamano & Satoshi Sato (2023): JENDL-5 benchmark test for shielding applications, Journal of Nuclear Science and Technology, DOI: 10.1080/00223131.2022.2164372

To link to this article: https://doi.org/10.1080/00223131.2022.2164372

Published online: 05 Feb 2023.

JOURNAL OF NUCLEAR SCIENCE AND TECHNOLOGY
https://doi.org/10.1080/00223131.2022.2164372

JENDL-5 benchmark test for shielding applications

Chikara Konno[a], Masayuki Ohta[b], Saerom Kwon[b], Seiki Ohnishi[c], Naoki Yamano[d] and Satoshi Sato[b]

[a]Nuclear Science and Engineering Center, Japan Atomic Energy Agency, Ibaraki, Japan; [b]Rokkasho Fusion Institute, National Institutes for Quantum Science and Technology, Aomori, Japan; [c]Department of Marine Risk Assessment, National Maritime Research Institute, Tokyo, Japan; [d]Laboratory for Zero-Carbon Energy, Tokyo Institute of Technology, Tokyo, Japan

ABSTRACT

JENDL-5 was validated from a viewpoint of shielding applications under the Shielding Integral Test Working Group of the JENDL Committee. The following benchmark experiments were selected: JAEA/FNS in-situ experiments, Osaka Univ./OKTAVIAN TOF experiments, ORNL/JASPER sodium experiments, NIST iron experiment and QST/TIARA experiments. These experiments were analyzed with MCNP and nuclear data libraries (JENDL-5, JENDL-4.0 or JENDL-4.0/HE, ENDF/B-VIII.0 and JEFF-3.3). The analysis results demonstrate that JENDL-5 is comparable to or better than JENDL-4.0 or JENDL-4.0/HE, ENDF/B-VIII.0 and JEFF-3.3 for neutron fluxes above 10 MeV in FNS in-situ iron experiment, neutron fluxes below 1 keV in FNS in-situ iron experiment, reaction rates of the ^{197}Au(n,γ)^{198}Au and ^{186}W(n,γ)^{187}W reactions in FNS in-situ copper experiment, neutron fluxes below 1 MeV in OKTAVIAN titanium experiment, neutron fluxes in OKTAVIAN manganese experiment, and neutron fluxes above 10 MeV in TIARA iron experiment.

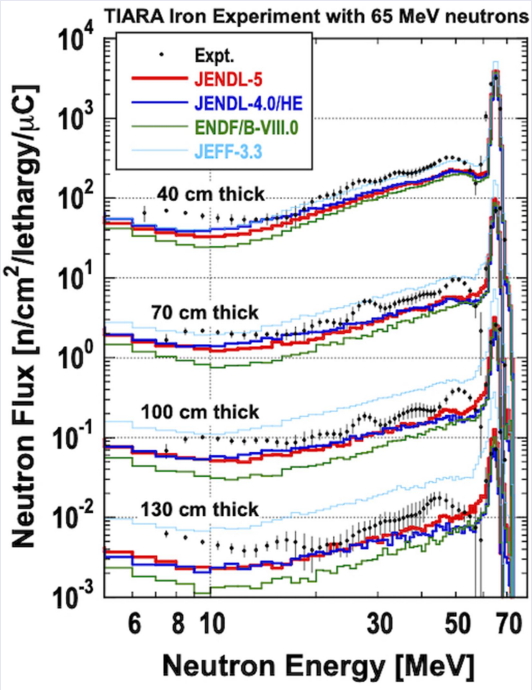

ARTICLE HISTORY
Received 6 September 2022
Accepted 26 December 2022

KEYWORDS
JENDL-5; shielding; benchmark test; MCNP; FNS; OKTAVIAN; JASPER; NIST; TIARA

1. Introduction

The Japanese Evaluated Nuclear Data Library, Version 5 [1] (JENDL-5) was released in December, 2021. It is essential to validate JENDL-5 with benchmark experiments. The Shielding Integral Test Working Group in the JENDL Committee (former Japanese Nuclear Data Committee (JNDC)) is in charge of validation work for JENDL through shielding benchmark tests and has validated JENDL-3 [2], JENDL-3.3 [3] and JENDL-4.0 [4] so far. Thus we have carried out the benchmark test of JENDL-5 for shielding applications under the Shielding Integral Test Working Group, while JENDL-5 benchmark tests for fission reactor applications are reported elsewhere [5]. Note that the target accuracy of this study is less than 20%, which may be acceptable for shielding applications.

CONTACT Chikara Konno konno.chikara@jaea.go.jp Nuclear Science and Engineering Center, Japan Atomic Energy Agency, 2-4 Shirakata, Tokai-mura, Naka-gun, Ibaraki 319-1195, Japan

Table 1. Reactions of measured reaction rates.

Reaction	Sensitive neutron
^{93}Nb(n,2n)$^{92\,m}$Nb	>10 MeV
^{27}Al(n,α)^{24}Na	>4 MeV
^{115}In(n,n′)$^{115\,m}$In	>0.5 MeV
^{186}W(n,γ)^{187}W	low energy
^{197}Au(n,γ)^{198}Au	low energy
^{235}U(n,fission)	low energy
^{238}U(n,fission)	>1 MeV

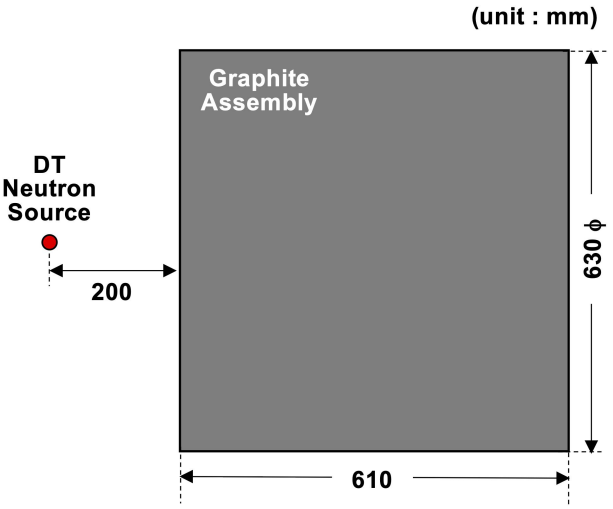

Figure 1. Experimental configuration of graphite in-situ experiment.

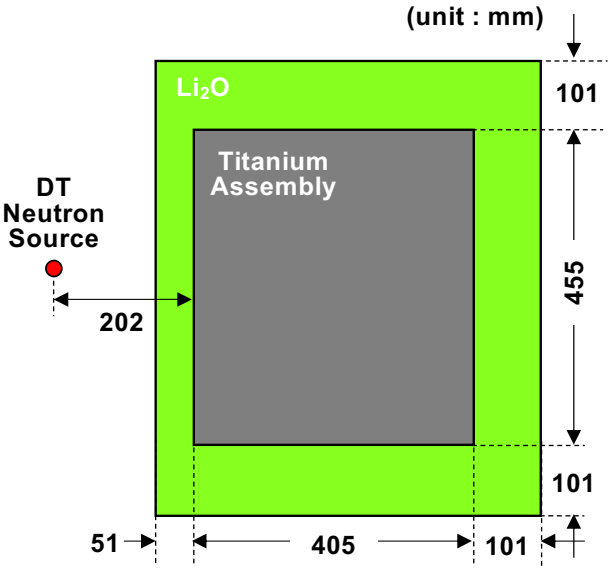

Figure 2. Experimental configuration of titanium in-situ experiment.

As the JENDL-5 benchmark test, we selected JAEA/FNS in-situ experiments [6–11], Osaka Univ./OKTAVIAN TOF experiments [12], ORNL/JASPER sodium experiments [13,14], NIST iron experiment [15] and QST/TIARA experiments [16,17], which were also used in the previous benchmark tests of JENDL. An evaluation scheme [18] of the shielding integral test for nuclear data libraries, which was

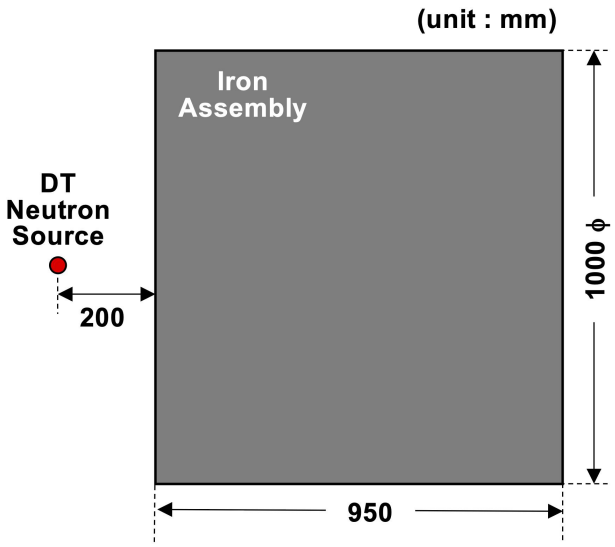

Figure 3. Experimental configuration of iron in-situ experiment.

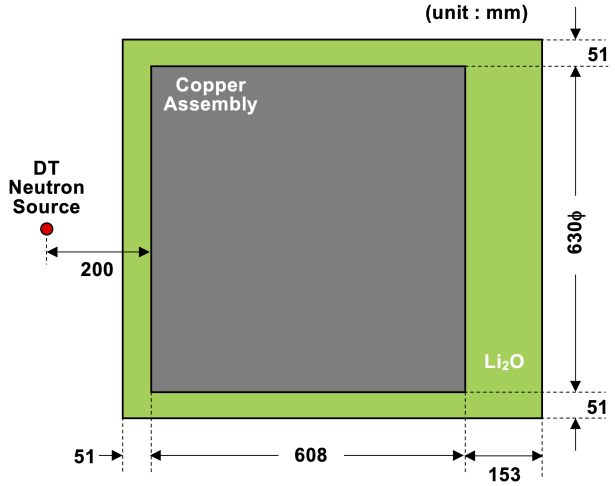

Figure 4. Experimental configuration of copper in-situ experiment.

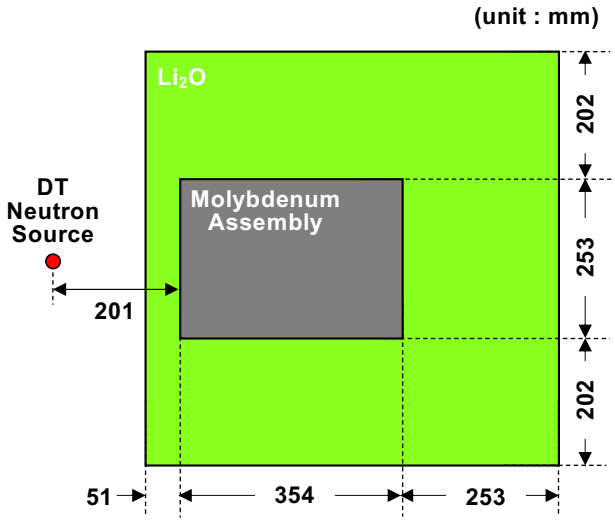

Figure 5. Experimental configuration of molybdenum in-situ experiment.

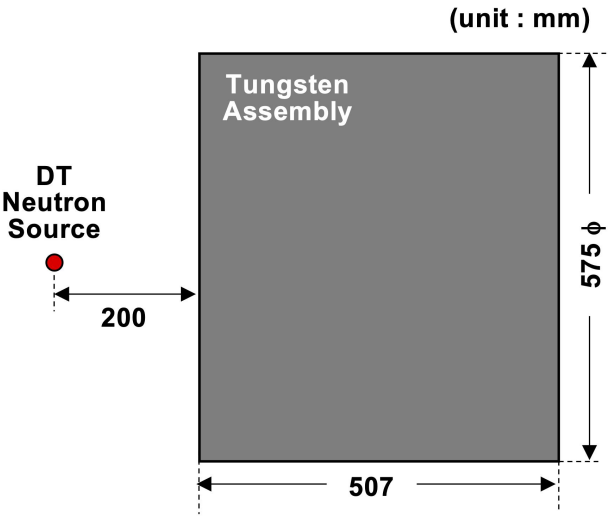

Figure 6. Experimental configuration of tungsten in-situ experiment.

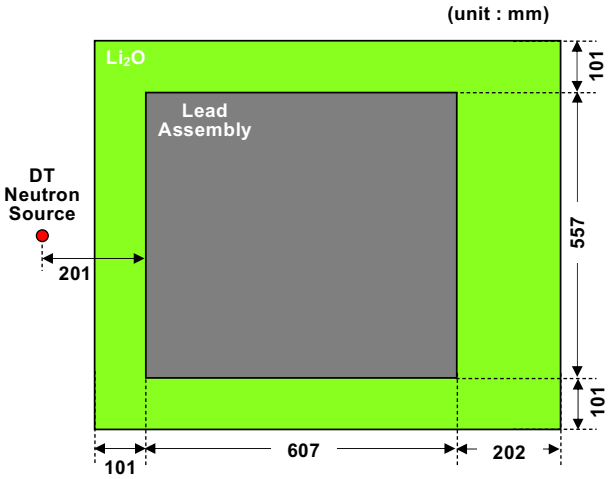

Figure 7. Experimental configuration of lead in-situ experiment.

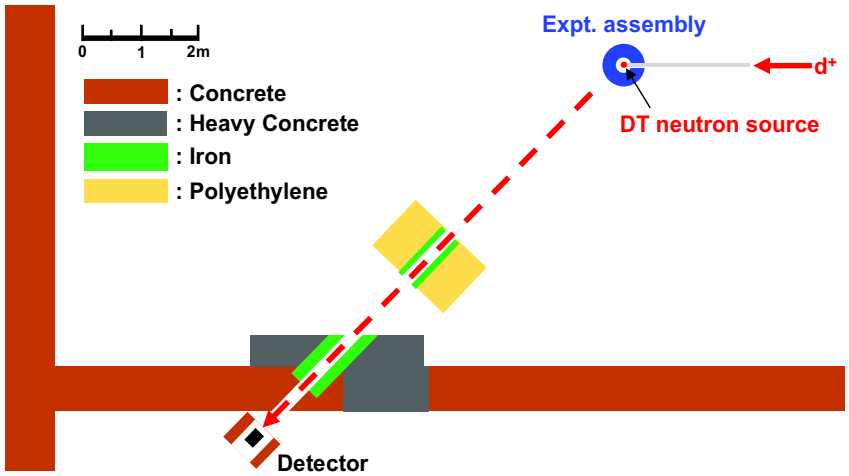

Figure 8. Experimental configuration of OKTAVIAN experiments.

established in JNDC, was also adopted in this benchmark test.

Section 2 describes brief descriptions of the selected shielding benchmark experiments. Section 3 presents analysis methods used in the benchmark test. Section 4 shows validation results of the benchmark experiments and discusses the results and issues to be solved. The concluding remarks are described in Section 5.

2. Overview of experiments

2.1. FNS experiments

The Fusion Neutronics Source (FNS) was an accelerator-based strong DT neutron source at Japan Atomic Energy Agency (JAEA). It was operated from 1981 to 2016 and a lot of various experiments, mainly benchmark experiments, were performed with the DT neutron source. In the benchmark experiments, neutron spectra were measured with a small NE213 scintillator of 14 mm in diameter, proton recoil counters and/or the slowing down time method, and reaction rates of the reactions shown in Table 1 were also measured with the activation foil method and micro fission chambers of ^{235}U and ^{238}U [6,8]. The following experiments were selected as this JENDL-5 benchmark test for shielding applications.

2.1.1. Graphite in-situ experiment

An integral experiment was carried out with a graphite assembly of 630 mm in effective diameter and 610 mm in thickness, which was set at 200 mm from the DT neutron source [6]. Figure 1 shows the experimental configuration. In this experiment, neutron spectra above 2 MeV, and reaction rates of

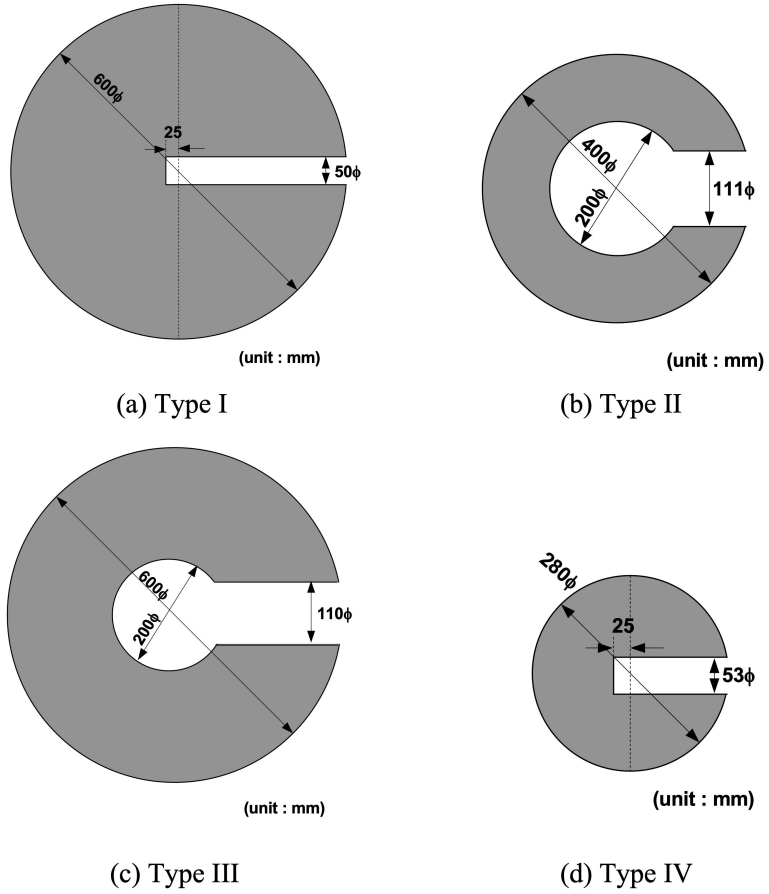

Figure 9. Four types of vessels in OKTAVIAN experiments.

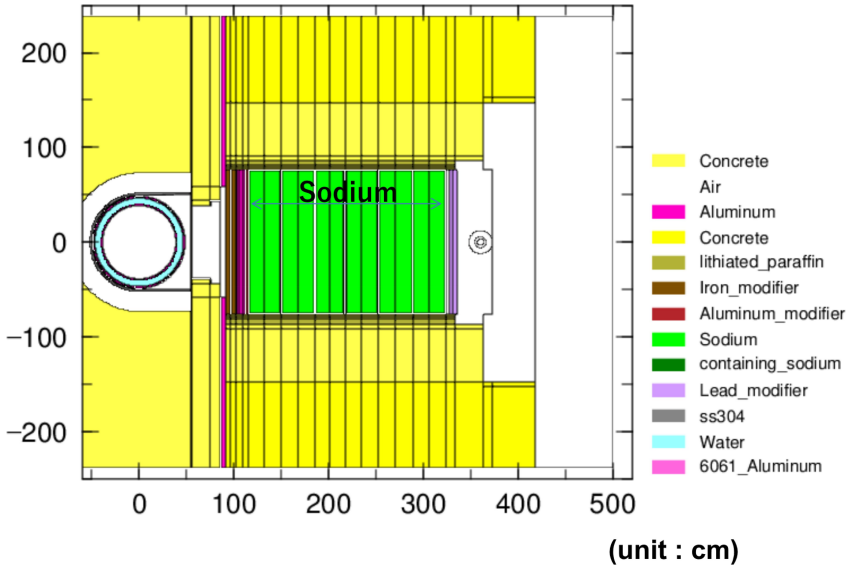

Figure 10. Experimental configuration of JASPER IVFS-IC/Pb.9 experiment.

several reactions were measured inside the assembly along the centerline.

2.1.2. *Titanium in-situ experiment*

An integral experiment on titanium [7] was performed with a titanium assembly of a rectangular shape of 455 mm × 455 mm × 405 mm, which was placed at the distance of 202 mm from the DT neutron source. The titanium assembly was furthermore covered with lithium oxide (Li_2O) in order to reduce an influence of background neutrons on the measurements inside the titanium assembly because the assembly was relatively small. The thicknesses of Li_2O were 51, 101 and 101 mm for the front, side and rear parts, respectively.

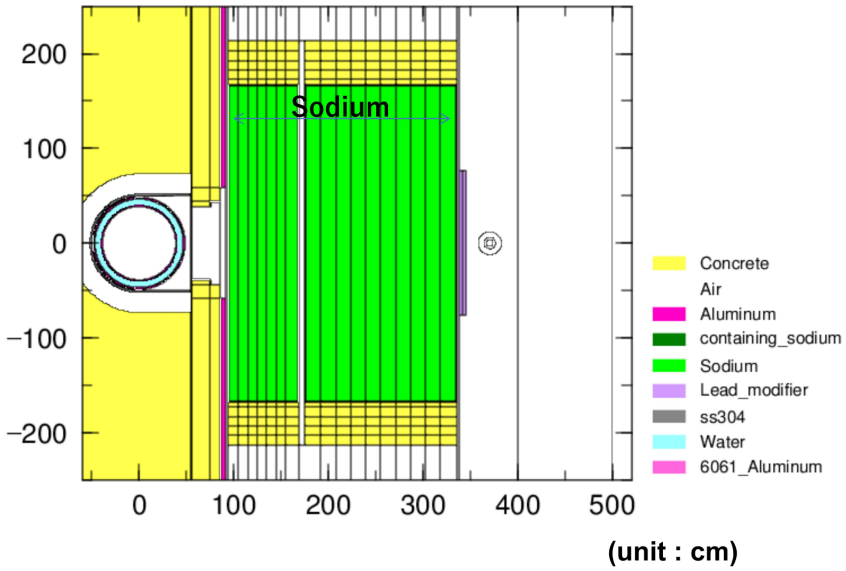

Figure 11. Experimental configuration of JASPER IHX-IB/Pb experiment.

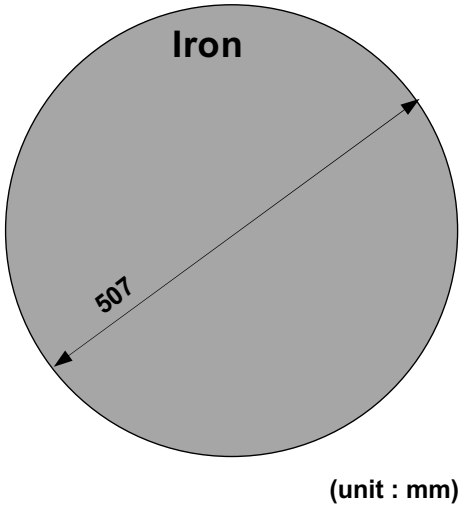

Figure 12. Experimental configuration of NIST experiment.

Table 2. Material density and vessel type.

Material	Material density [g/cm^3]	Vessel type
LiF	1.79	I
CF_2	1.30	II
Al	1.22	II
Si	1.29	III
Ti	1.54	II
Cr	3.72	II
Mn	4.37	I
Co	1.94	II
Cu	6.23	I
As	3.09	II
Se	2.29	II
Zr	2.84	I
Nb	4.39	IV
Mo	2.15	I
W	4.43	II

Figure 2 shows the experimental configuration. Reaction rates of several reactions were measured inside the assembly along the centerline.

2.1.3. Iron in-situ experiment

An integral experiment was carried out with an iron assembly of 1000 mm in diameter and 950 mm in thickness, which was set at 200 mm from the DT neutron source [8]. Figure 3 shows the experimental configuration. In this experiment, neutron spectra covering almost the whole energy above 1 eV and reaction rates of several reactions were measured inside the assembly along the centerline.

2.1.4. Copper in-situ experiment

An integral experiment with a copper assembly of a quasi-cylinder of 315 mm in radius and 608 mm in depth was performed [9]. It was covered with additional Li_2O layers of 51, 51 and 153 mm in thickness for the front, side and rear parts, respectively, to reduce scattering neutrons into the assembly from a concrete wall of the experimental room. Figure 4 shows the experimental configuration. Reaction rates of several reactions were measured inside the assembly along the centerline.

2.1.5. Molybdenum in-situ experiment

An integral experiment on molybdenum was performed [10]. A rectangular molybdenum assembly of 253 mm × 253 mm × 354 mm was used in the experiment. The molybdenum assembly was placed at the distance of 201 mm from the DT neutron source. The molybdenum assembly was also covered with 51, 202, and 253 mm thick Li_2O blocks for the front, side, and rear parts, respectively, to eliminate background neutrons. Figure 5 shows the experimental configuration. Reaction rates of several reactions were measured inside the assembly along the centerline.

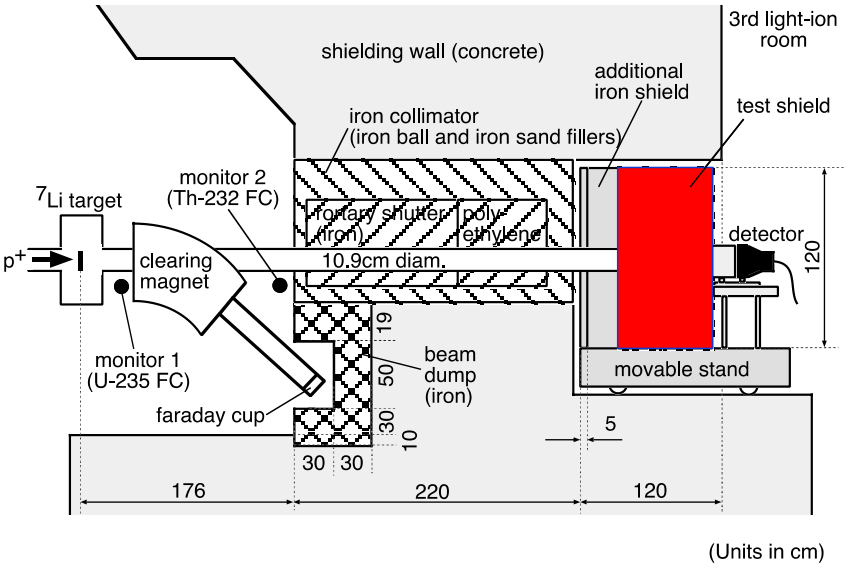

Figure 13. Experimental configuration of TIARA experiments.

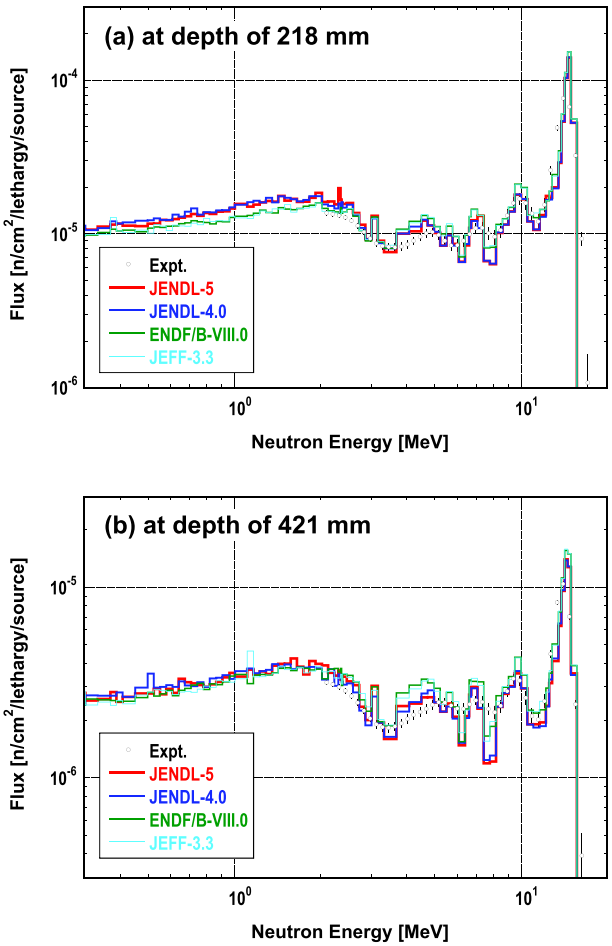

Figure 14. Neutron spectra in graphite in-situ experiment.

2.1.6. Tungsten in-situ experiment

An integral experiment was carried out with a tungsten assembly of 575 mm in effective diameter and 507 mm in thickness, which was set at 200 mm from the DT neutron source [8]. Figure 6 shows the experimental configuration. In this experiment, neutron spectra above 5 keV and reaction rates of several reactions were measured inside the assembly along the centerline.

2.1.7. Lead in-situ experiment

An integral experiment with a lead assembly of 557 mm in width and in height and 607 mm in thickness was carried out [11]. The lead assembly was set at 201 mm from the DT neutron source and was also covered with Li_2O blocks (101 mm in thickness for the front and side parts, 202 mm in thickness for the rear part of the assembly) for excluding background neutrons from the concrete wall. Figure 7 shows the experimental configuration. Reaction rates of several reactions were measured inside the assembly along the centerline.

2.2. OKTAVIAN experiments

Sphere pile integral experiments were carried out with the DT neutron source facility OKTAVIAN in Osaka University from 1984 to 1988 [12]. Leakage neutron current spectra above 100 keV from the spherical piles were measured with the TOF technique, where the flight pass was about 11 m. The neutron detector used was a cylindrical liquid organic scintillator NE-218. Figure 8 shows the experimental configuration. The piles were stainless-steel spherical hollow vessels filled with powder or flakes of LiF, CF_2, Al, Si, Ti, Cr, Mn, Co, Cu, As, Se, Zr, Nb, Mo and W. Four types of

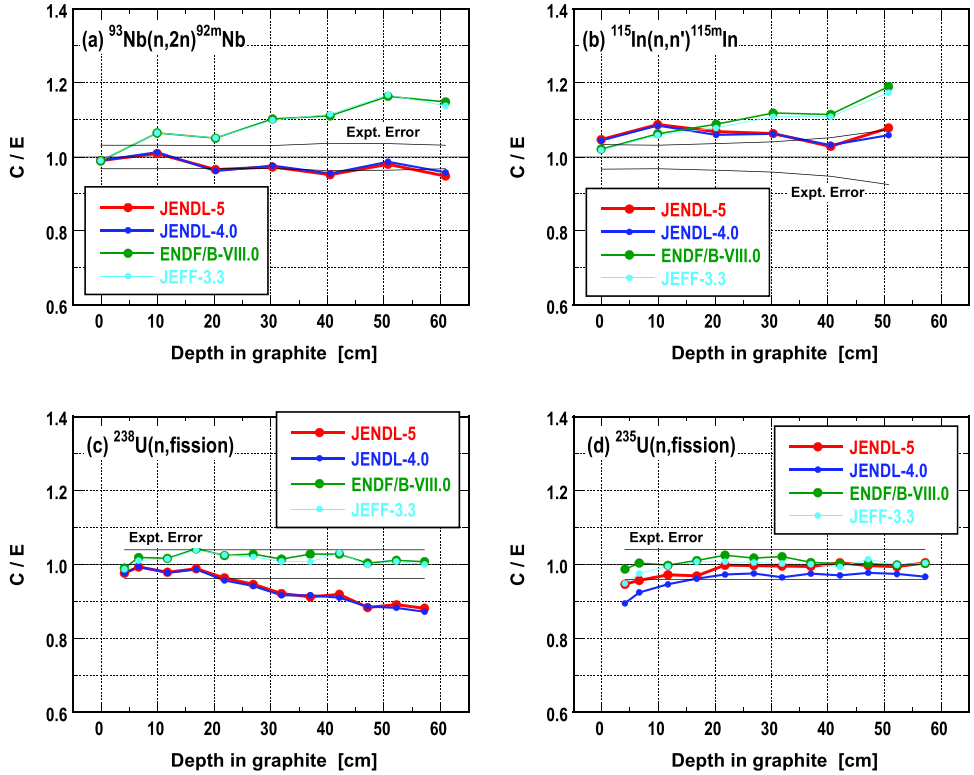

Figure 15. C/Es of reaction in graphite in-situ experiment.

vessels shown in Figure 9 were used. Table 2 summarizes the material densities and vessel types for the materials.

2.3. JASPER sodium experiments

A series of experiments were performed as the US and Japan Shielding Program for Experimental Research (JASPER) of fast breeding reactor (FBR) shielding mockups. Various types of benchmark experiments were conducted for simulating FBR shield. In this study, we selected two typical sodium benchmark experiments because the material configurations were rather simple and thick enough to investigate deep penetration. The selected experiments were JASPER IVFS-IC/Pb.9 (197.4 cm thick sodium) [13] and JASPER IHX-IB/Pb (231.3 cm thick sodium) [14].

The neutron source of the JASPER experiments was a neutron beam collimated with two collimators (front one was 15 and 7/16 inches in radius and rear one was 17 and 3/32 inches in radius) from the Tower Shielding Reactor II of Oak Ridge National Laboratory in the U.S. To reduce air-scattering neutrons the reactor and detector were shielded with lead and lithium-paraffin (IVFS-IC) or concrete (IHX-IB) and the reactor neutron beam was tightly collimated. The sodium sample was a rectangular form with stainless-steel container and placed so that its axis coincided with the axis of the neutron beam. The detector was placed just behind the sample. Figures 10 and 11 show the experimental configurations. Neutron spectra between 800 keV and 15 MeV were measured by using an NE213 scintillator. Spherical proton recoil counters, filled with hydrogen to pressures of 1, 3, and 10 atmospheres, were also used to measure neutron spectra between 50 keV and 1 MeV. Bonner ball counters from 3 to 10 inches were also used to measure Bonner ball count rates. The response data of the Bonner ball counters in Ref [19] were used for our analyses. The measured data with each detector were normalized to the reactor power (watts) using the data from two fission chambers positioning along the reactor centerline.

2.4. NIST iron experiment

In the 1980s, a problem was known that the discrepancy between predicted and observed neutron transport results was more than 30% in deep penetration calculations. Therefore, a benchmark experiment was performed at the National Institute of Standards and Technology (NIST) [15]. In this experiment, an encapsulated ^{252}Cf

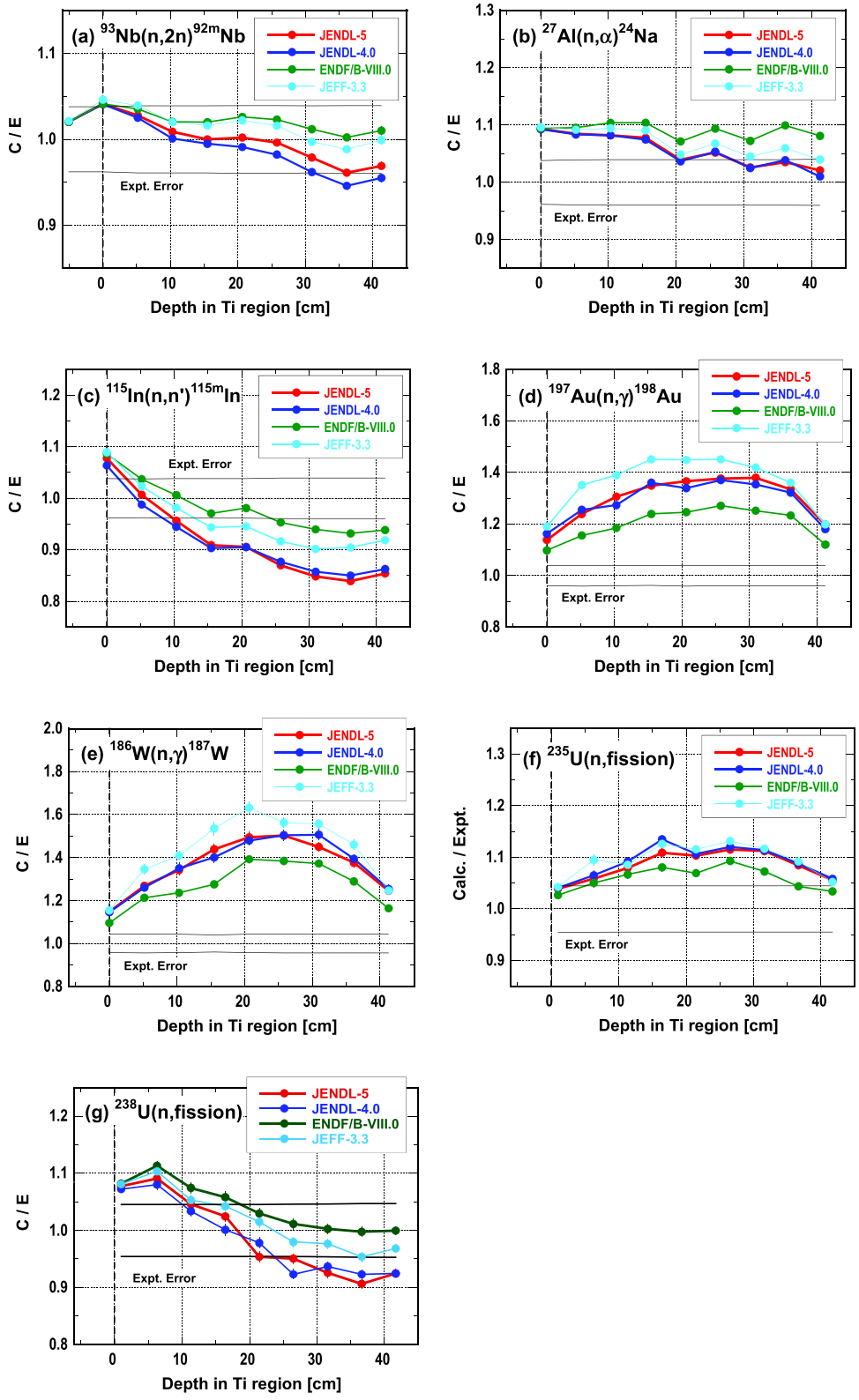

Figure 16. C/Es of reaction in titanium in-situ experiment.

spontaneous fission neutron source, whose neutron intensity error was estimated to be 1%, from the National Bureau of Standards (NBS) [20] was placed at the center of an iron sphere of 507 mm in diameter, and a leakage neutron spectrum from the sphere was measured with proton recoil counters. Figure 12 shows the experimental configuration.

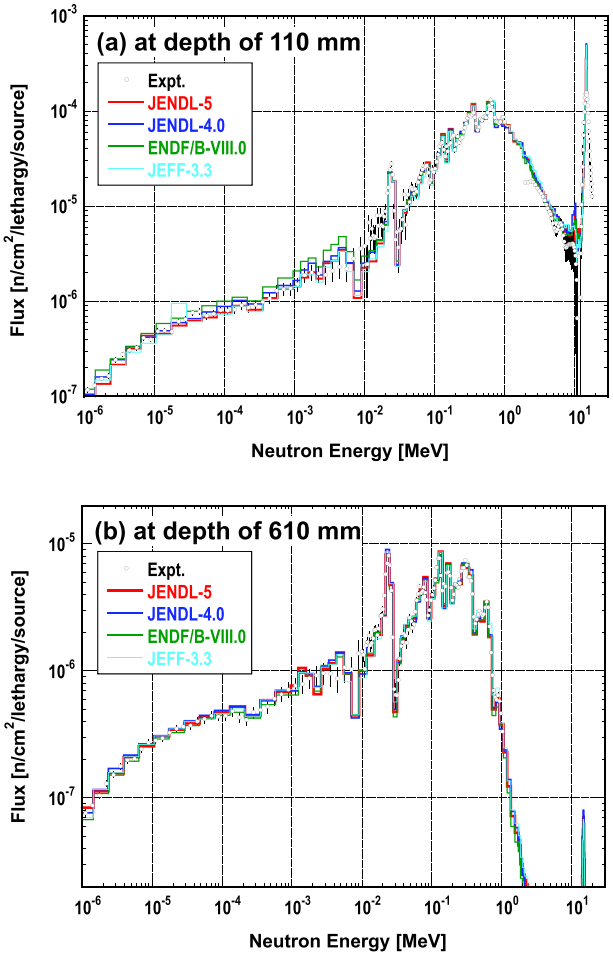

Figure 17. Neutron spectra in iron in-situ experiment.

2.5. TIARA experiments

Iron and Concrete shielding experiments [16,17] were carried out with quasi-mono energetic neutrons of 40 and 65 MeV at TIARA (Takasaki Ion Accelerators for Advanced Radiation Application) of QST (National Institutes for Quantum Science and Technology), which was formerly affiliated in JAERI (Japan Atomic Energy Research Institute). These neutrons were produced by bombarding 43 and 68 MeV protons to a solid Lithium-7 target and was collimated by an iron rotary shutter and polyethylene. The collimated neutrons irradiated an iron or concrete test shield and spectra of the penetrated neutrons above 10 MeV were measured with a BC501A scintillator just behind the shield. Figure 13 shows the experimental configuration.

3. Analysis method

The benchmark experiments described in Section 2 were analyzed with the Monte Carlo code, MCNP4.3c [21] for the JASPER sodium experiments or MCNP6.2 [22] for the other experiments, and JENDL-5. The nuclear data libraries of JENDL-4.0 [23] (or JENDL-4.0/HE [24] only for the TIARA experiments), ENDF/B-VIII.0 [25] and JEFF-3.3 [26] were also used for comparison. The official ACE files [27–31] of these nuclear data libraries were used in the analyses except for JENDL-5 above 20 MeV, whose ACE files were processed with NJOY2016.65 [32] modified for JENDL-5. Note that the ^{1}H file of JENDL-5 was adopted in the analyses with ENDF/B-VIII.0 of the TIARA concrete experiments because the ^{1}H file of ENDF/B-VIII.0 was up to 20 MeV. For the same reason the ^{1}H and ^{28}Si files of JENDL-5 were adopted in the analyses with JEFF-3.3 of the TIARA concrete experiments. The dosimetry reaction cross section data for the reaction rate calculations were taken from the JENDL dosimetry file 99 [33]. We did not use the thermal scattering law (TSL) data of JENDL-5 except for the FNS graphite in-situ experiment because the TSL data affected little impact on the analysis results. The details of the analyses are described in Refs [3,4,7–11,34].

4. Results and discussion

In this section the calculated results are compared with the measured ones for each experiment. We validate JENDL-5 from the comparisons. We also try to investigate reasons that JENDL-5 is better than JENDL-4.0 or JENDL-4.0/HE and issues of the other nuclear data libraries. This investigation is limited and is not perfect, but we believe that it will be useful to the future study.

4.1. FNS experiments

4.1.1. Graphite in-situ experiment

Figure 14 shows the neutron spectra above 300 keV at the depths of 218 and 421 mm. The calculated neutron spectra with JENDL-5 and JENDL-4.0 are almost the same and agree with the measured ones, while those with ENDF/B-VIII.0 and JEFF-3.3 are slightly different from those with JENDL-5 and JENDL-4.0. The ratios of the calculated reaction rates to the experimental ones (C/E) of typical reactions are shown in Figure 15. All the calculated reaction rates agree with the measured ones within approximately 20%. Note that the C/Es have two clear trends: i) JENDL-5 and JENDL-4.0, ii) ENDF/B-VIII.0 and JEFF-3.3.

4.1.2. Titanium in-situ experiment

Figure 16 shows the C/Es for the reaction rates: (a) ^{93}Nb(n,2n)^{92m}Nb, (b) ^{27}Al(n,α)^{24}Na, (c) ^{115}In(n,n')^{115m}In, (d) ^{197}Au(n,γ)^{198}Au, (e) ^{186}W(n,γ)^{187}W, (f) ^{235}U(n,fission) and (g) ^{238}U(n,fission). The position of the front surface of the titanium region is taken as 0 cm in these figures. Note that

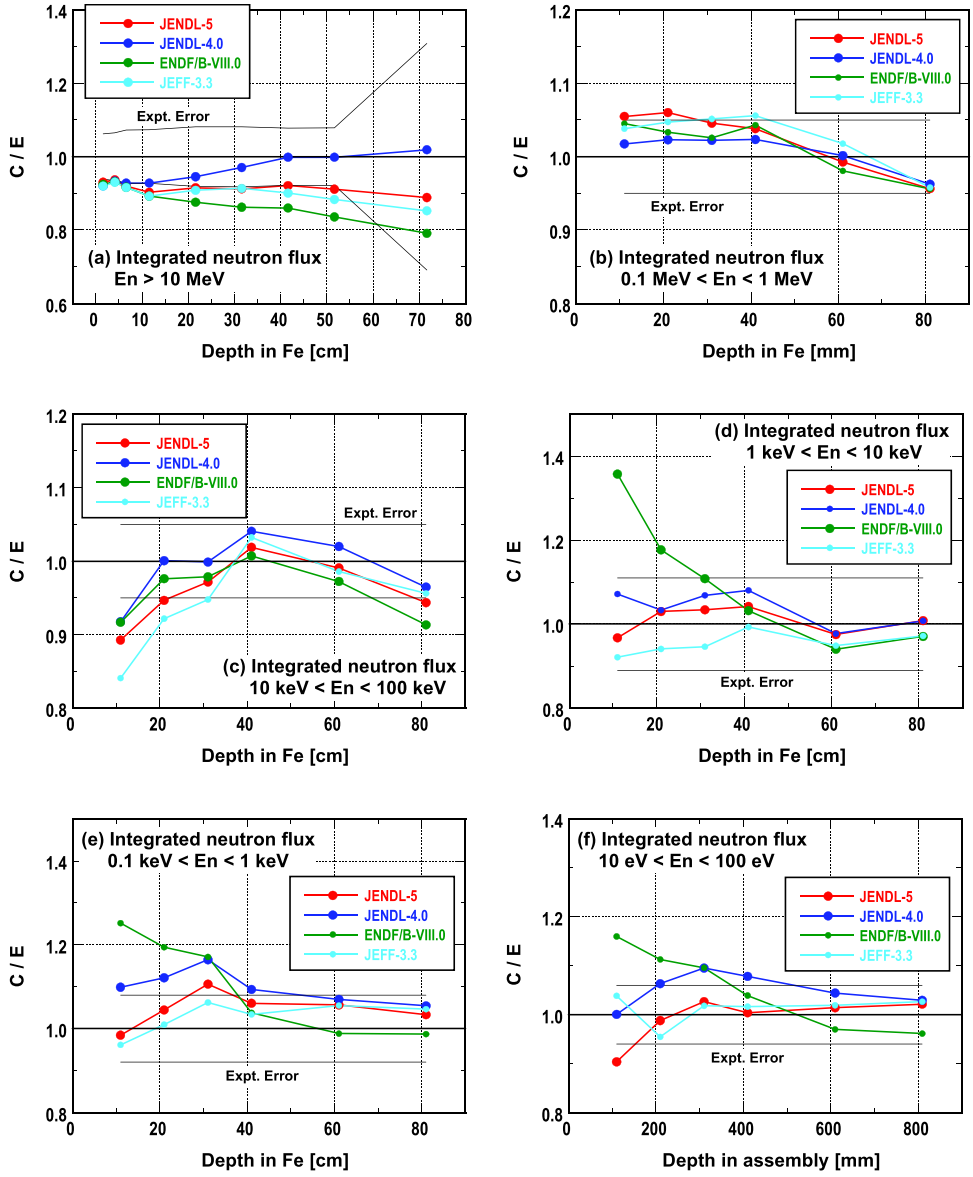

Figure 18. C/Es of integrated neutron fluxes for specified energy regions in iron in-situ experiment.

the negative position is in the front of Li_2O region. All the calculated results are slightly scattered. The calculated results with JENDL-5 are comparable to those with JENDL-4.0, although most of the JENDL-5 data are re-evaluated. Note that all the calculated reaction rates of the ^{197}Au(n,γ)^{198}Au and ^{186}W(n,γ)^{187}W reactions overestimate the measured ones.

4.1.3. Iron in-situ experiment

Figure 17 shows the neutron spectra above 1 eV at the depths of 110 and 610 mm. The calculated neutron spectra with JENDL-5, JENDL-4.0 and JEFF-3.3 are almost the same though the iron data in JENDL-5 were re-evaluated independently to those in JENDL-4.0. They agree with the measured ones but that with ENDF/B-VIII.0 overestimates the measured one below 10 keV at the depth of 110 mm. In order to examine this issue, the C/Es of integrated neutron fluxes for specific energy regions are shown in Figure 18. The calculated neutron fluxes with JENDL-5 and JEFF-3.3 agree the measured ones better than those with JENDL-4.0 and ENDF/B-VIII.0. The problem of ENDF/B-VIII.0 which overestimates the neutron fluxes below 10 keV is investigated in Ref [35], where it is specified that the inelastic scattering data of ^{56}Fe in ENDF/B-VIII.0 causes the problem.

4.1.4. Copper in-situ experiment

The C/Es of typical reaction rates are shown in Figure 19. The C/Es of the reaction rates of the threshold reactions, particularly ^{93}Nb(n,2n)^{92m}Nb, have different trends corresponding to the nuclear data libraries used. The calculated reaction rates of the non-threshold reactions, ^{197}Au(n,γ)^{198}Au and ^{186}W(n,γ)^{187}W, with JENDL-5 are in much better agreement with the measured ones than those with the other nuclear data

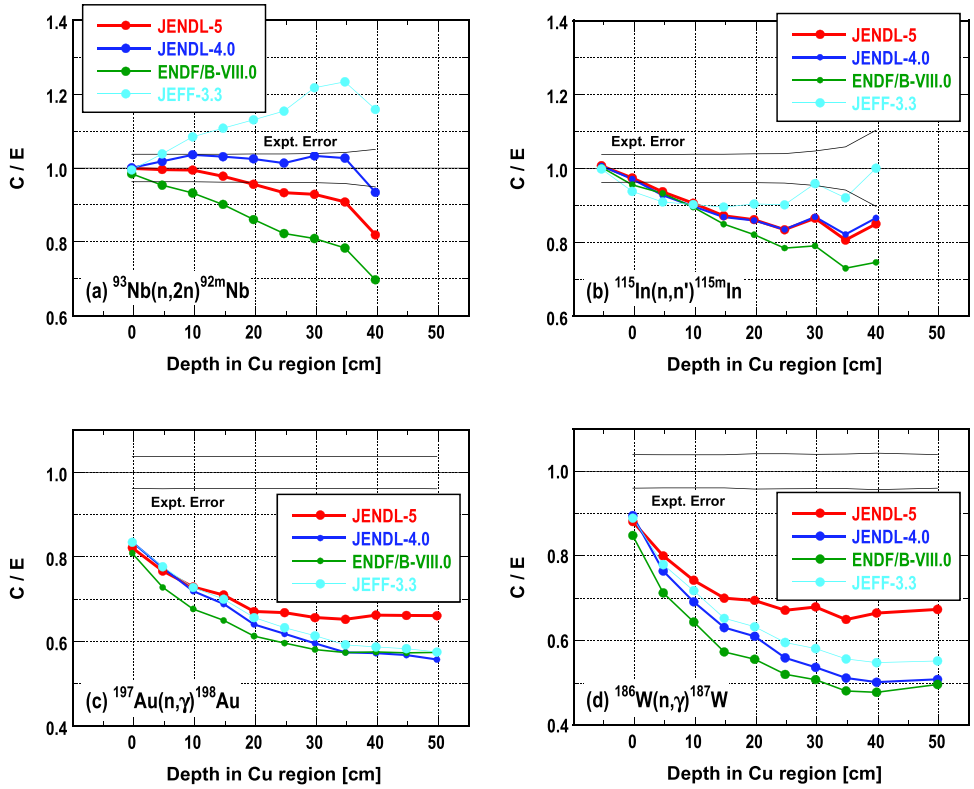

Figure 19. C/Es of reaction rates in copper in-situ experiment.

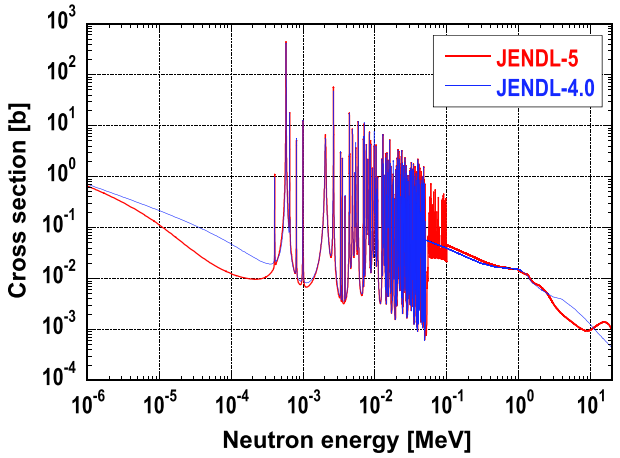

Figure 20. Capture cross section of ^{63}Cu.

libraries, though they still underestimate the measured ones. This is due to the modification of the cross section of the ^{63}Cu(n,γ) reaction in JENDL-5 (see Figure 20).

4.1.5. Molybdenum in-situ experiment

Figure 21 shows the C/Es for the reaction rates: (a) ^{93}Nb(n,2n)^{92m}Nb, (b) ^{27}Al(n,α)^{24}Na, (c) ^{115}In(n,n')^{115m}In, (d) ^{197}Au(n,γ)^{198}Au, (e) ^{186}W(n,γ)^{187}W, (f) ^{235}U(n,fission) and (g) ^{238}U(n,fission). The front surface of the molybdenum region is taken as 0 cm in the depth. The calculated results with JENDL-5 were almost the same as those with JENDL-4.0. On the whole, the C/Es gradually decrease with increasing the depth in the molybdenum region. The results with JEFF-3.3 have a similar tendency to those with JENDL-5 and JENDL-4.0, while those with ENDF/B-VIII.0 are somewhat different from those with the other libraries.

4.1.6. Tungsten in-situ experiment

Figure 22 shows the neutron spectra above 5 keV at the depths of 76 and 380 mm. The calculated neutron spectra with JENDL-5 and JENDL-4.0 are almost the same and agree with the measured ones, while those with ENDF/B-VIII.0 and JEFF-3.3 are slightly different from those with JENDL-5 and JENDL-4.0. The C/Es of typical reaction rates are shown in Figure 23. All the calculated reaction rates agree with the measured ones within approximately 20%.

4.1.7. Lead in-situ experiment

The several C/E plots for the reaction rates are shown in Figure 24. The calculated reaction rate of the ^{93}Nb(n,2n)^{92m}Nb reaction with JENDL-5 is almost the same as those with JENDL-4.0 and JEFF-3.3 and agrees with the measured one. All the calculated reaction rates for the ^{115}In(n,n')^{115m}In reaction tend to underestimate. The underestimation with JENDL-5

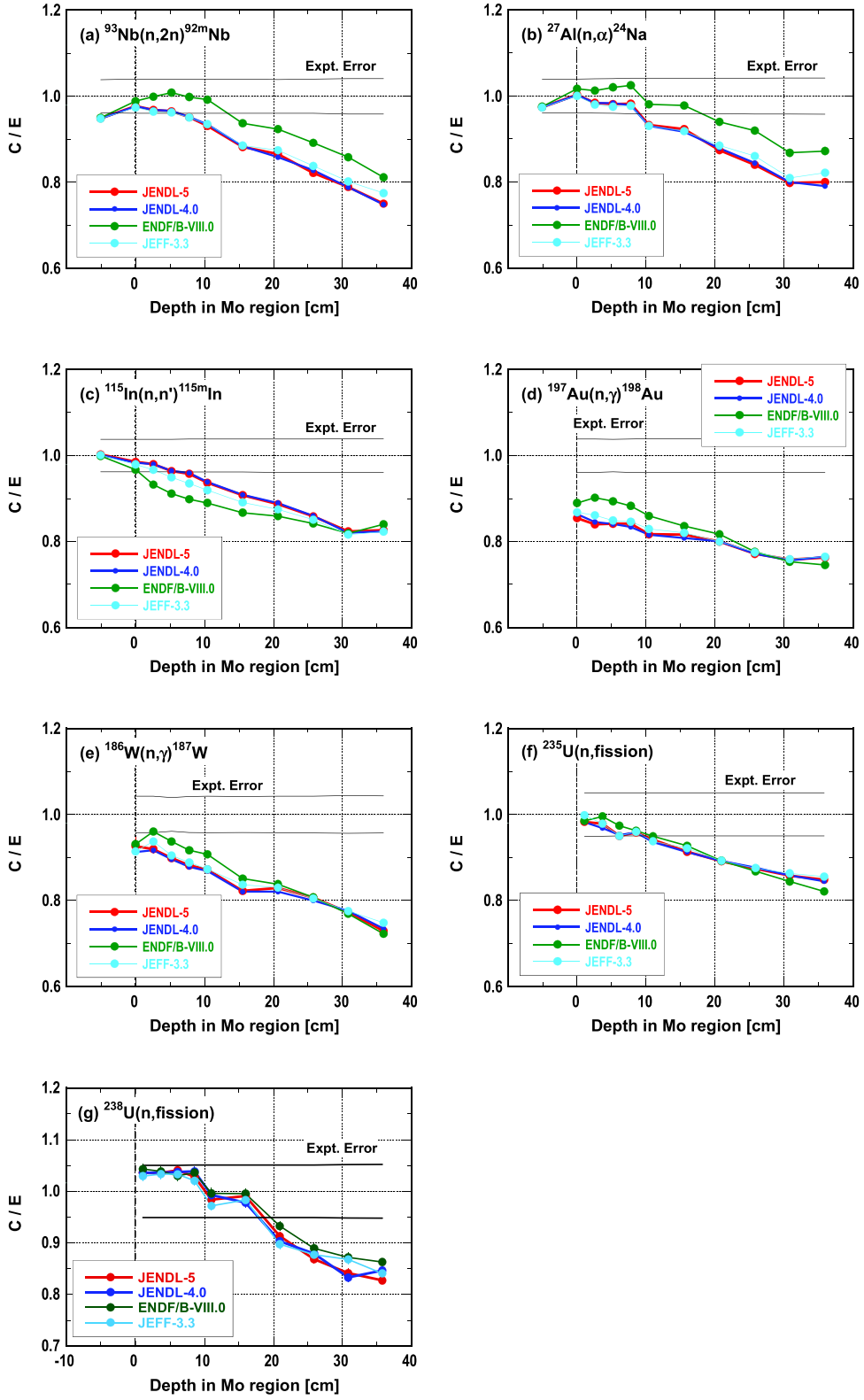

Figure 21. C/Es of reaction rates in molybdenum in-situ experiment.

is improved compared with that with JENDL-4.0. All the calculated reaction rates of the non-threshold reactions, ^{197}Au(n,γ)^{198}Au and ^{186}W(n,γ)^{187}W, are almost the same and tend to underestimate the measured ones.

4.2. OKTAVIAN experiments

We selected the Si, Ti, Cr, Mn, Co, Cu, Nb, and W experiments from the view of shielding application. The measured and calculated neutron current spectra

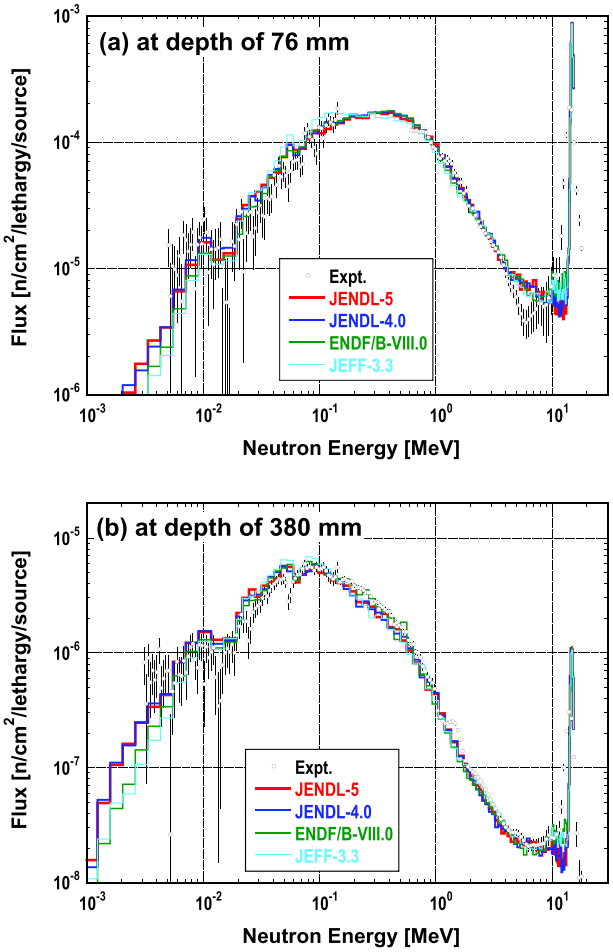

Figure 22. Neutron spectra in tungsten in-situ experiment.

are shown with the C/Es of integrated neutron currents of 0.1–0.5 MeV, 0.5–1 MeV, 1–5 MeV, 5–10 MeV and beyond 10 MeV in Figures 25a and 25b. The followings are found from Figures 25a and 25b.

- Si, Cr and W : The calculation result with JENDL-5 is almost the same as that with JENDL-4.0.
- Ti : The calculation result with JENDL-4.0 overestimates the measured neutron fluxes below 1 MeV. JENDL-5 improves the overestimation at a similar level with ENDF/B-VIII.0 and JEFF-3.3.
- Mn : The calculation result with JENDL-4.0 overestimates the measured neutron fluxes above 0.1 MeV, while that with JENDL-5 agrees with the measured neutron flux well and is comparable to those with ENDF/B-VIII.0 and JEFF-3.3.
- Co : All the calculation results corresponds to the measured neutron flux above 10 MeV well, but they underestimate the measured neutron flux from 1 MeV to 10 MeV and overestimate the measured neutron flux below 1 MeV. The calculated neutron flux below 0.5 MeV with JENDL-5 agrees with the measured one better than that with JENDL-4.0, while the calculated neutron flux from 0.5 to 1 MeV with JENDL-5 is worse than that with JENDL-4.0.
- Cu : The calculation result with JENDL-5 is almost the same as that with JENDL-4.0, but it is slightly better and worse for the neutron fluxes above 10 MeV and from 5 to 10 MeV, respectively. Note that the calculation result with ENDF/B-VIII.0 overestimates the neutron flux

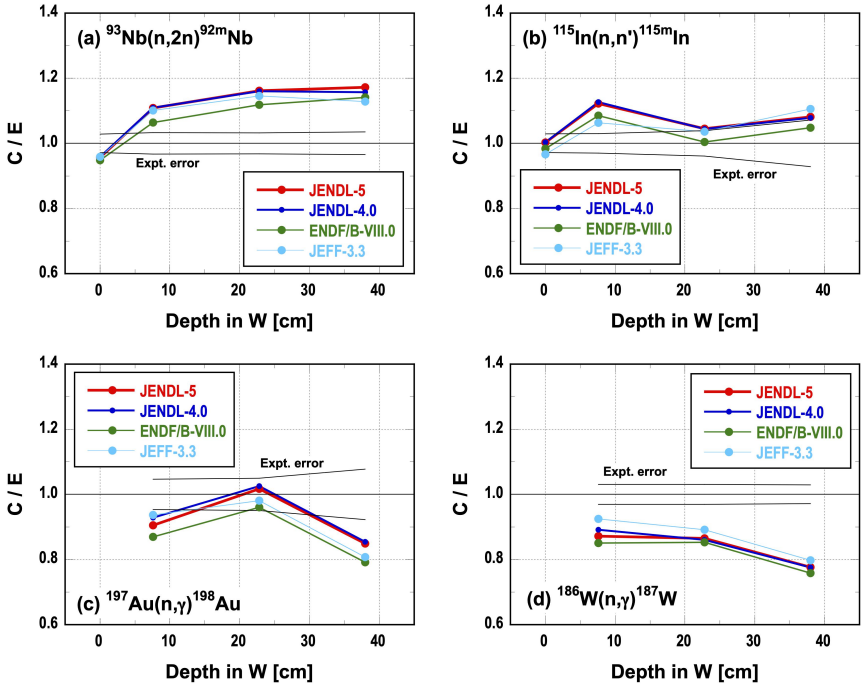

Figure 23. C/Es of reaction rates in tungsten in-situ experiment.

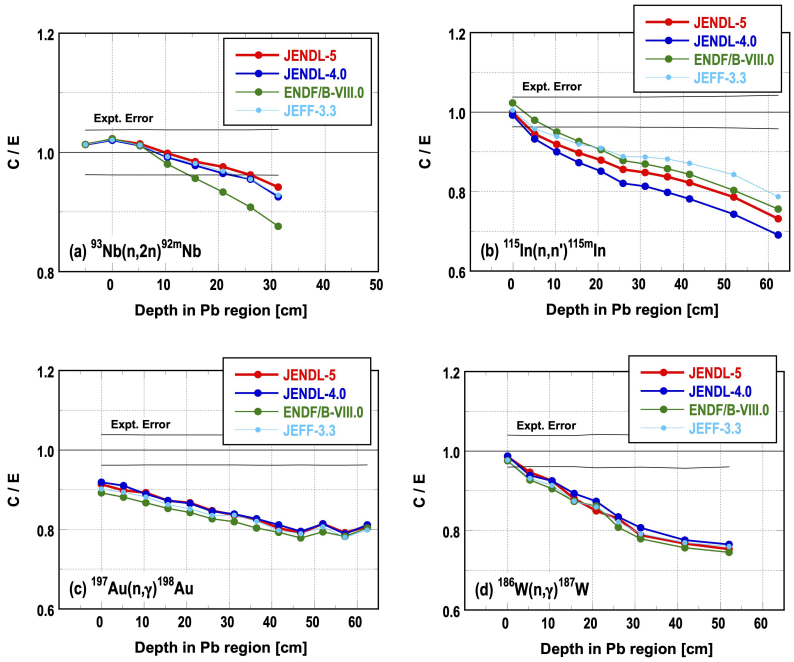

Figure 24. C/Es of reaction rates in lead in-situ experiment.

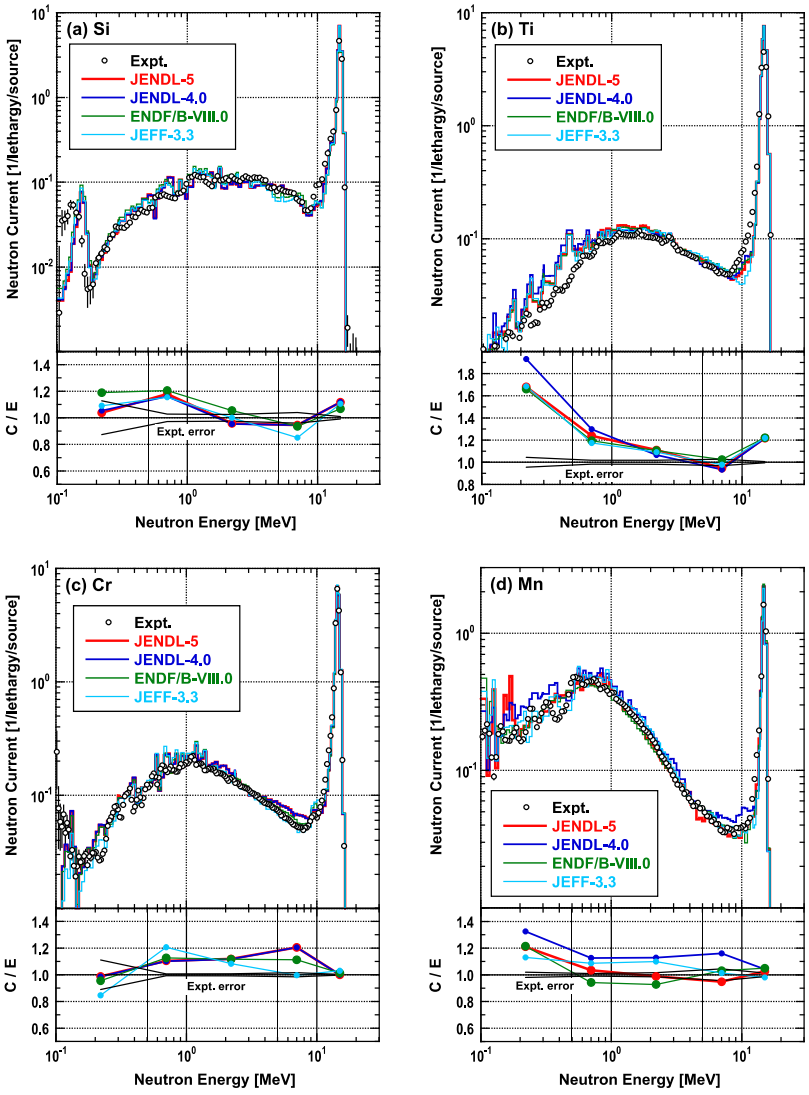

Figure 25a. Neutron spectra and C/Es of integrated neutron currents in OKTAVIAN experiments.

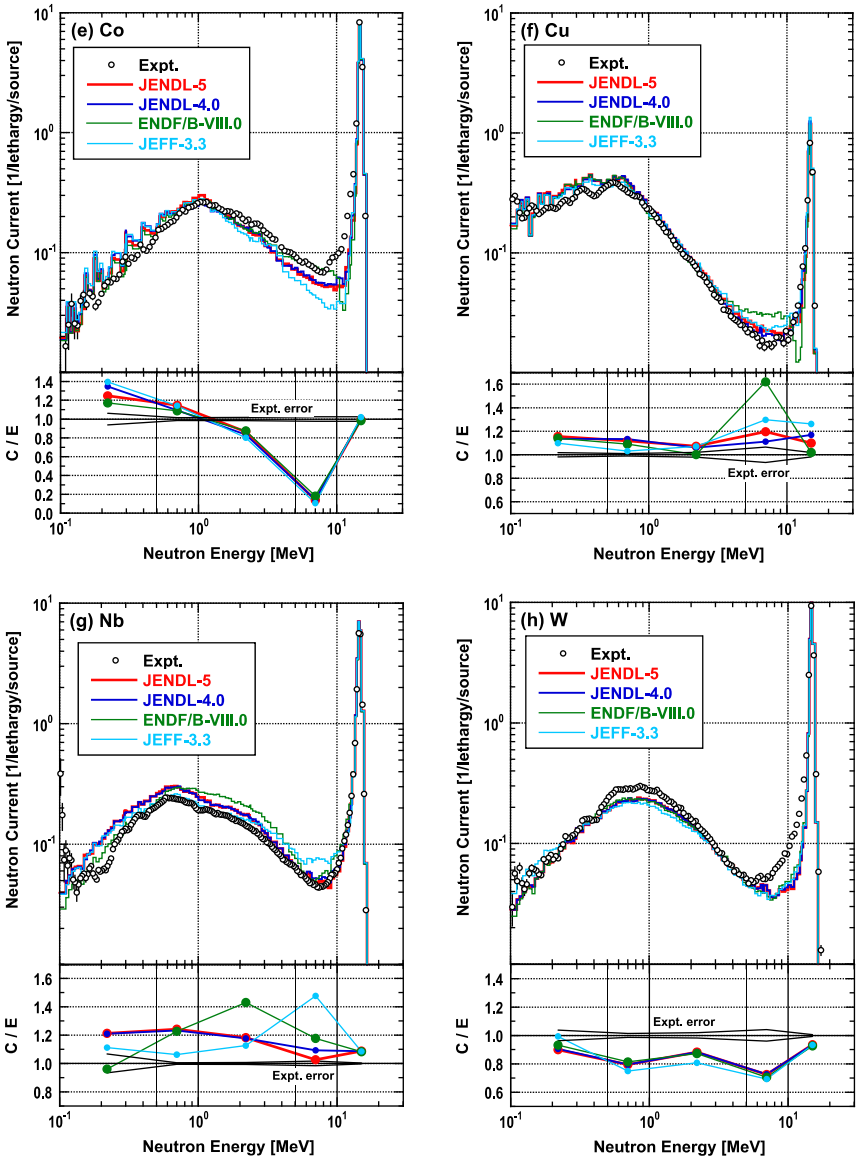

Figure 25b. Continued.

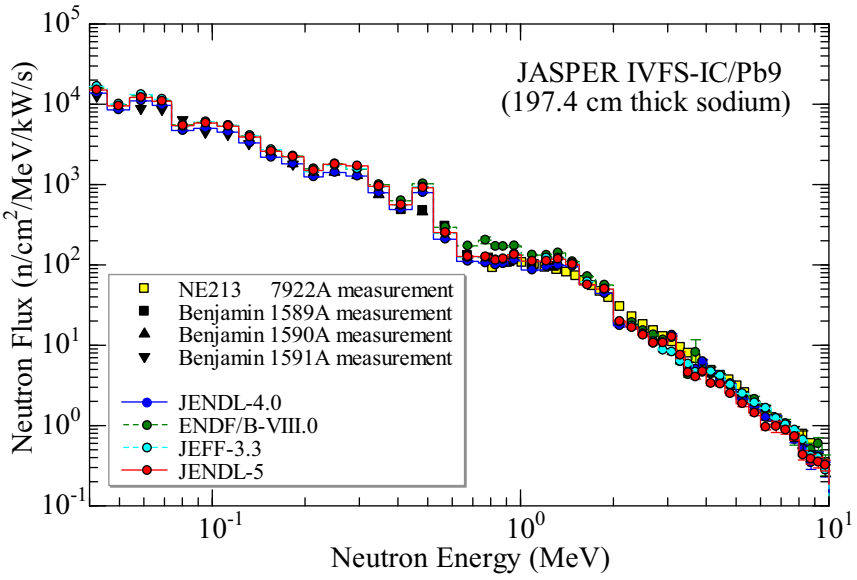

Figure 26. Neutron spectra in JASPER IVFS-IC/Pb.9 experiment.

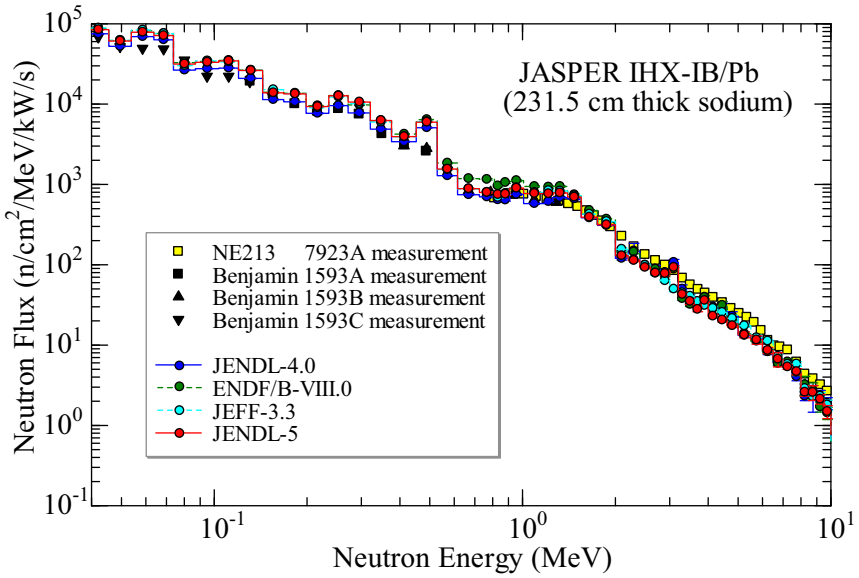

Figure 27. Neutron spectra in JASPER IHX-IB/Pb experiment.

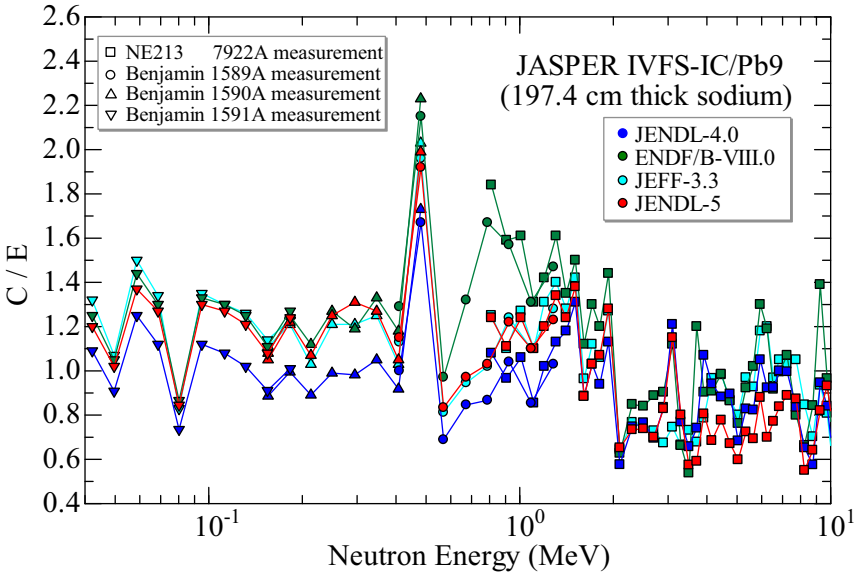

Figure 28. C/Es of the neutron fluxes in JASPER IVFS-IC/Pb.9 experiment.

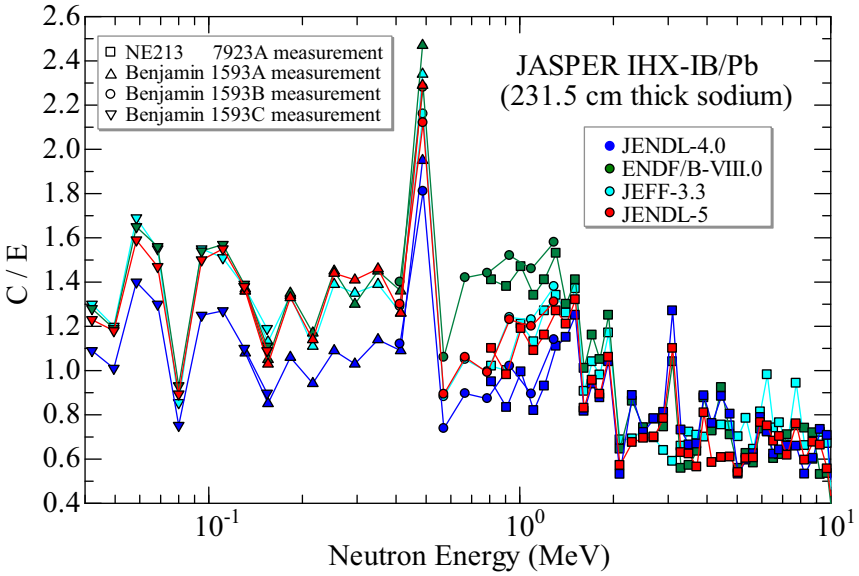

Figure 29. C/Es of the neutron fluxes in JASPER IHX-IB/Pb experiment.

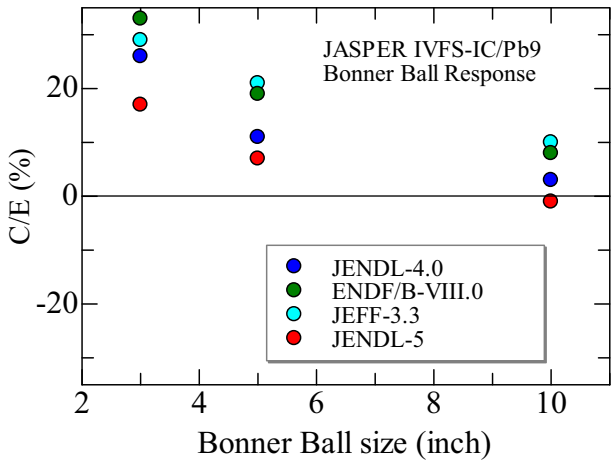

Figure 30. C/Es of Bonner Ball count rates in JASPER IVFS-IC/Pb.9 experiment.

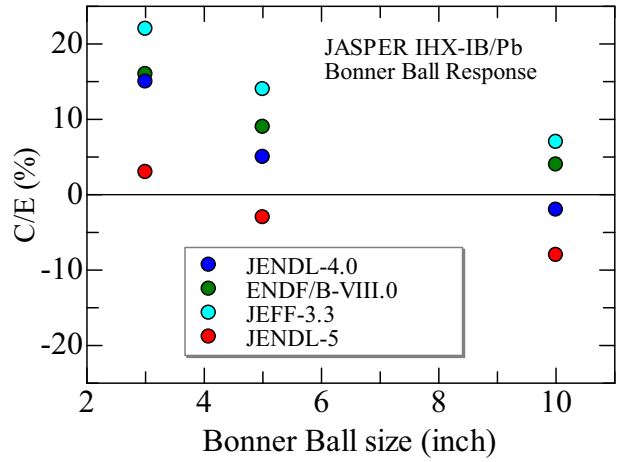

Figure 31. C/Es of Bonner Ball count rates in JASPER IHX-IB/Pb experiment.

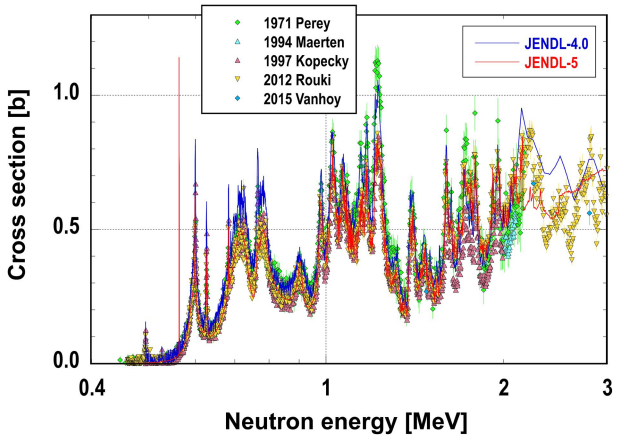

Figure 32. Comparison of ^{23}Na inelastic scattering cross section.

from 5 to 10 MeV very much and that with JEFF-3.3 overestimates the neutron flux above 5 MeV.

- Nb : The calculation result with JENDL-5 improves only the neutron flux from 5 to 10 MeV. Those with ENDF/B-VIII.0 and JEFF-3.3 overestimate the neutron flux from 1 to 5 MeV and from 5 to 10 MeV, respectively.

4.3. JASPER sodium experiments

The neutron spectra in the JASPER IVFS-IC/Pb.9 and IHX-IB/Pb experiments are also shown in Figures 26 and 27, respectively. The C/E values of the neutron fluxes in the JASPER IVFS-IC/Pb.9 and IHX-IB/Pb experiments are also shown in Figures 28 and 29, respectively. The results with JENDL-5 indicate a good agreement with both the measurements, while those with ENDF/B-VIII.0 slightly show overestimations compared with the measurements in the energy range between 550 keV and 1.5 MeV. The calculation results are consistent each other and the tendency of the penetrated neutron energy spectra is the same between the IVFS-IC/Pb.9 and the IHX-IB/Pb experiments. The C/E results of the Bonner Ball count rates are shown in Figures. 30 and 31, respectively. Those with JENDL-5 indicate a good agreement with the measurements for the Bonner Ball counters of 3, 5 and 10 inches in diameter compared with those with JENDL-4.0. The results with ENDF/B-VIII.0 and JEFF-3.3 overestimate the experiments more than those with JENDL-5.

The difference is attributed to the cross section of the inelastic scattering and the angular distribution of the elastic scattering of ^{23}Na. Figure 32 shows the inelastic scattering cross section with experimental data [36–40]. JENDL-5 is evaluated with reference to the recent measurement [39], while JENDL-4.0 is larger below 2 MeV. Figure 33 shows the angular distribution of the elastic scattering at the incident neutron energies of 550 keV and 1 MeV with experimental data [38,41]. The angular distributions at 550 keV are similar between JENDL-4.0 and JENDL-5 but the forward scattering is enhanced at 1 MeV in JENDL-5.

4.4. NIST iron experiment

Figure 34 shows the calculated neutron current spectra on the NIST iron sphere surface with JENDL-5, JENDL-4.0, JEFF-3.3, and ENDF/B-VIII.0 with the measured one. Note that the current spectra are integrated over the whole surface. All of the calculation results reproduce the measured one.

For a quantitative comparison, the spectra are partially integrated over specific energies. Figure 35 shows the C/Es of the integrated neutron currents. The calculated statistical errors are small enough. The C/Es range from 0.77 to 1.07, and all the calculation results agree well with the experimental ones in the energy region below 1

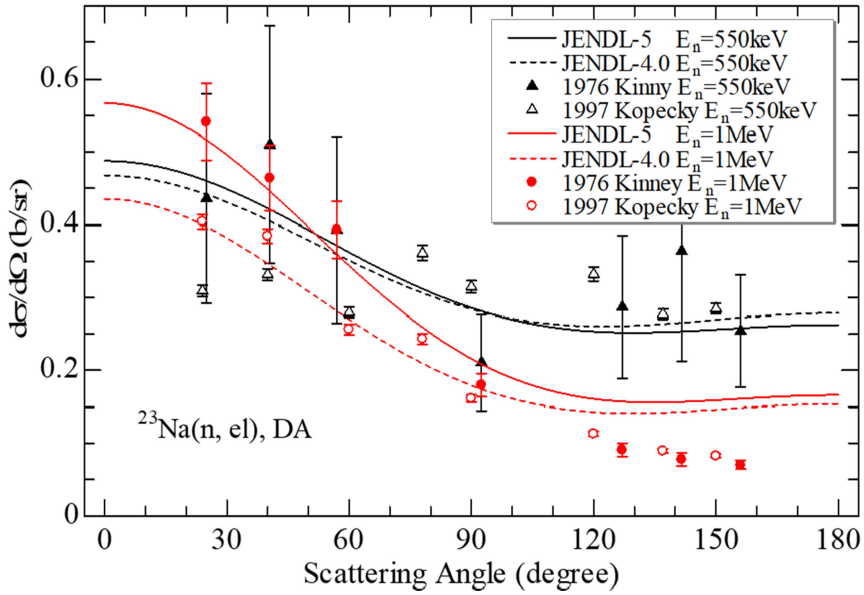

Figure 33. Comparison of ^{23}Na angular distribution of elastic scattering.

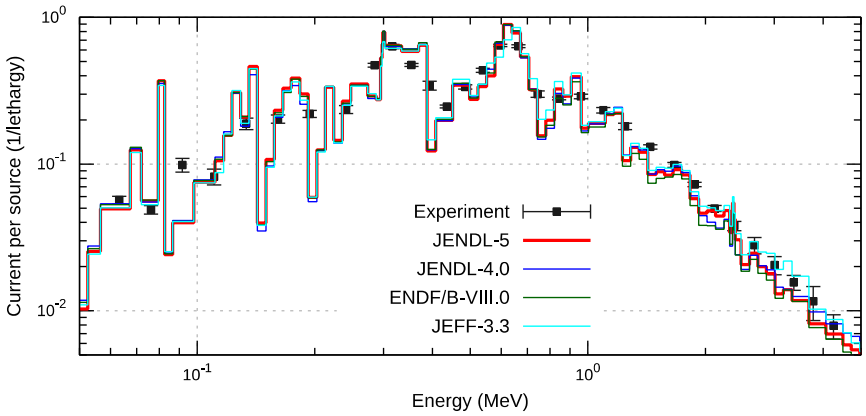

Figure 34. Neutron spectra in NIST iron experiment.

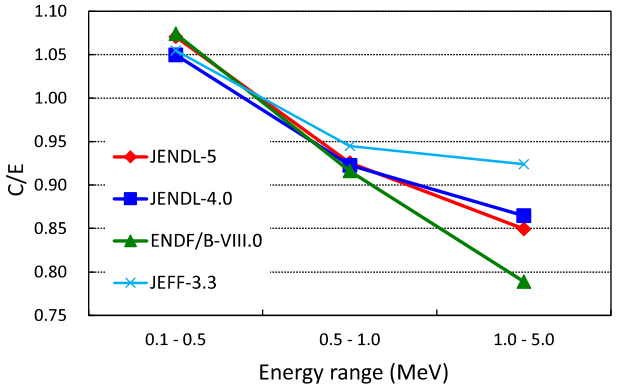

Figure 35. C/Es of integrated neutron currents in NIST iron experiment.

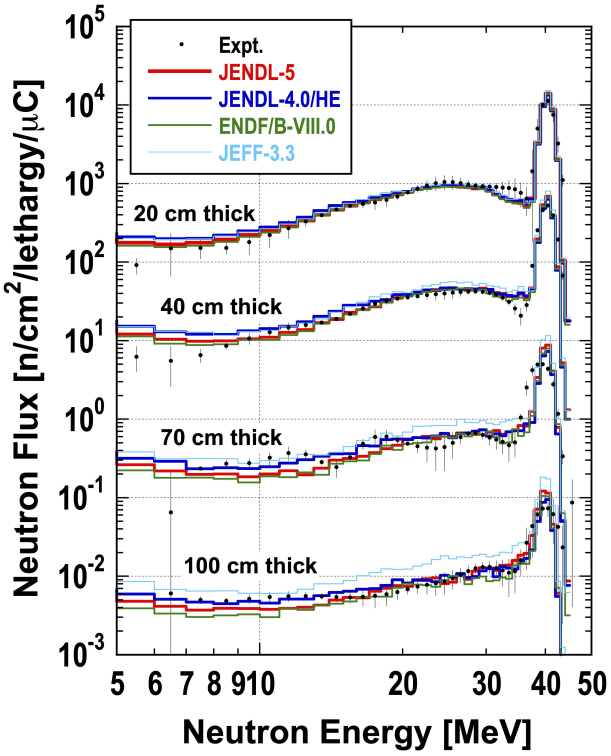

Figure 36. Neutron spectra in TIARA iron experiment with 40 MeV neutrons.

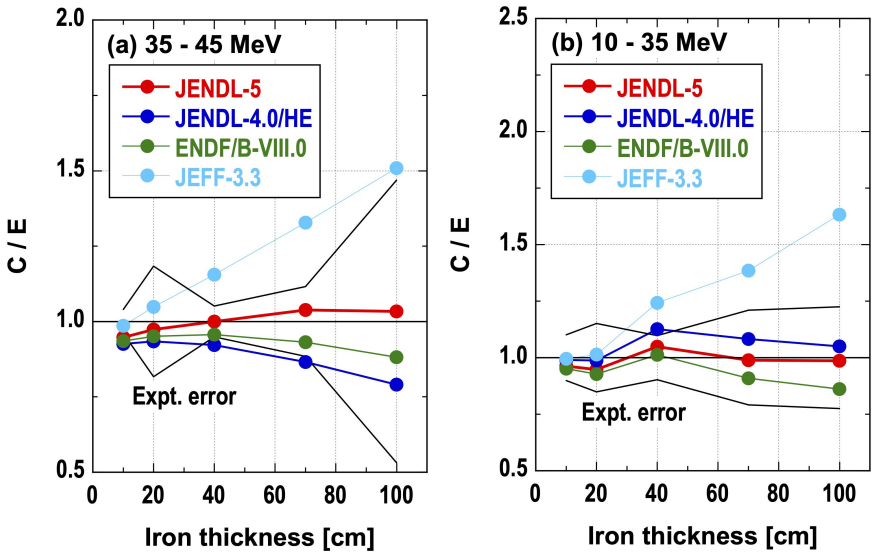

Figure 37. C/Es of integrated neutron fluxes in TIARA iron experiment with 40 MeV neutrons.

MeV. It is noted that the result with ENDF/B-VIII.0 tends to underestimate more in the higher energy region.

4.5. TIARA experiments

4.5.1. Iron experiment with 40 MeV neutrons

Figure 36 shows the measured and calculated neutron spectra in the iron experiment with 40 MeV neutrons. The calculated spectra with JEFF-3.3 overestimate the measured ones for the thicker iron shield. On the other hand, those with JENDL-5, JENDL-4.0/HE and ENDF/B-VIII.0 show a better agreement with the measured ones. In order to compare the measured and calculated neutron spectra in detail, the C/Es of integrated neutron fluxes of 35–45 MeV and 10–35 MeV are shown in Figure 37. The calculated neutron fluxes with JENDL-5 show the best agreement with the measured ones in both the energy regions.

4.5.2. Iron experiment with 65 MeV neutrons

Figure 38 shows the measured and calculated neutron spectra in the iron experiment with 65 MeV neutrons. The C/Es of integrated neutron fluxes of 60–70 MeV

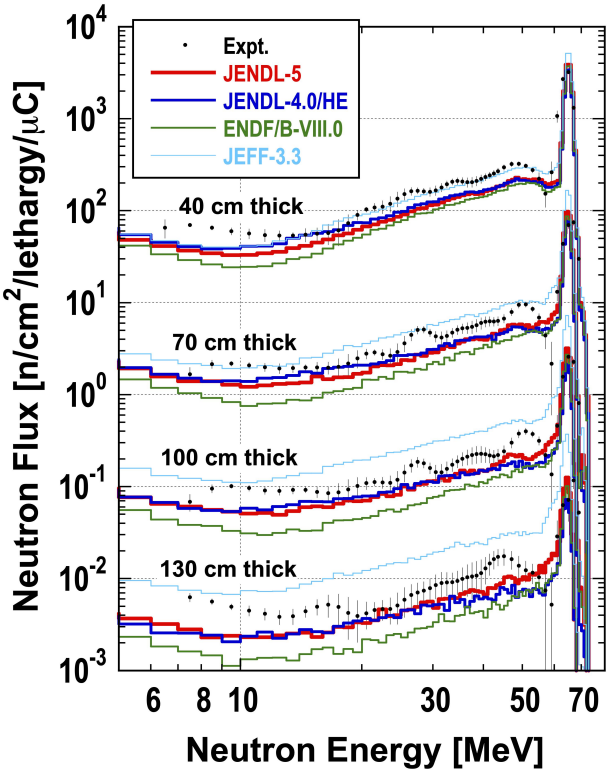

Figure 38. Neutron spectra in TIARA iron experiment with 65 MeV neutrons.

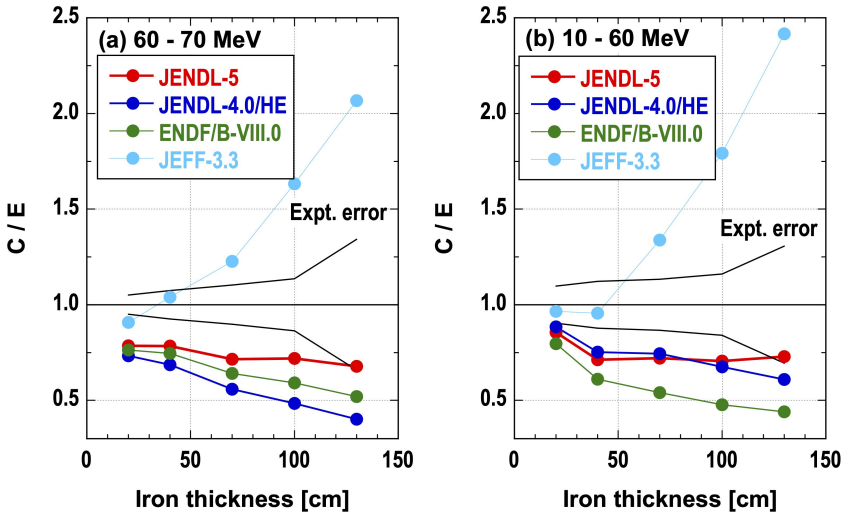

Figure 39. C/Es of integrated neutron fluxes in TIARA iron experiment with 65 MeV neutrons.

and 10–60 MeV regions are shown in Figure 39. The calculated spectra with JENDL-5 underestimate the measured ones, which oscillate due to the unfolding issue, but they agree with the measured ones the best. The overestimation tendency of the calculated spectra with JEFF-3.3 is enhanced more than that in the experiment with 40 MeV neutrons. The calculated neutron spectra with ENDF/B-VIII.0 underestimate the measured ones more with increasing the iron thickness. The C/Es of neutron flux of 10–60 MeV with JENDL-4.0/HE are almost the same as those with JENDL-5, while those of 60–70 MeV with JENDL-4.0/HE are much smaller for the thicker iron than those with JENDL-5. It is considered that this improvement in JENDL-5 is mainly due to revision of the elastic scattering and non-elastic scattering cross sections of ^{56}Fe from those in JENDL-4.0/HE as shown in Figure 40.

4.5.3. Concrete experiment with 40 MeV neutrons

Figures 41 and 42 show the measured and calculated neutron spectra and the C/Es of integrated neutron fluxes of 35–45 MeV and 10–35 MeV in the concrete experiment with 40 MeV neutrons, respectively. The calculated neutron fluxes with

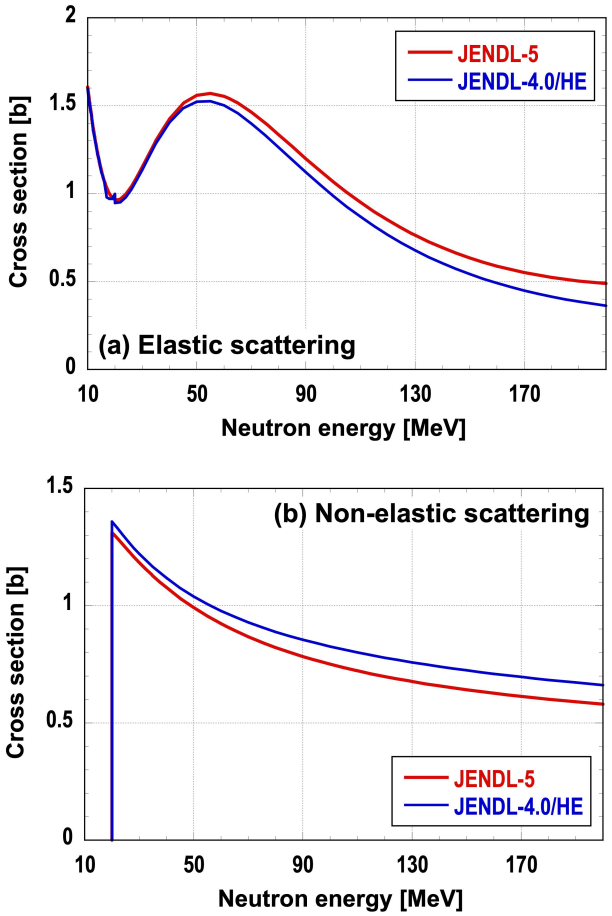

Figure 40. Cross sections of elastic scattering and non-elastic scattering above 10 MeV in ^{56}Fe.

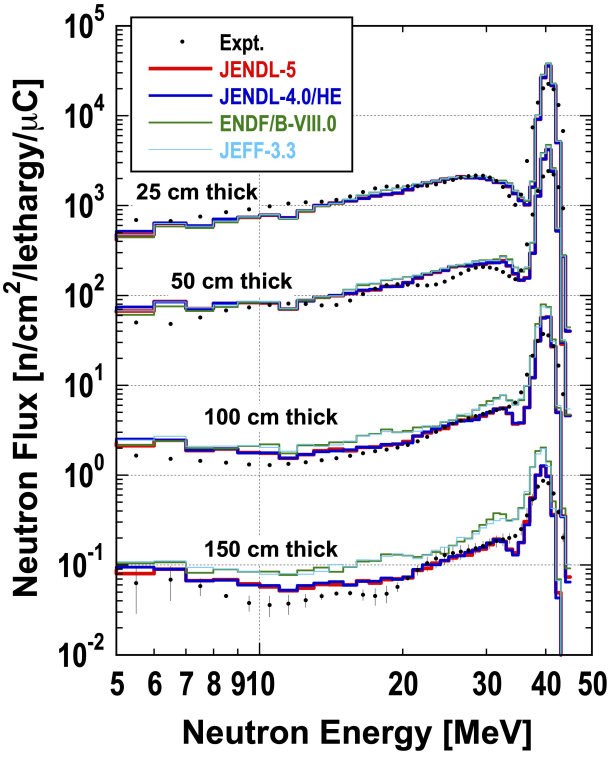

Figure 41. Neutron spectra in TIARA concrete experiment with 40 MeV neutrons.

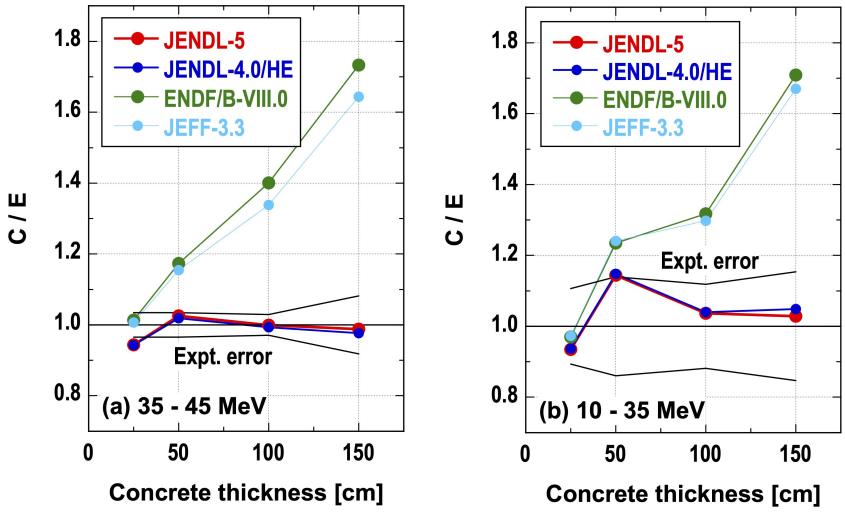

Figure 42. C/Es of integrated neutron fluxes in TIARA concrete experiment with 40 MeV neutrons.

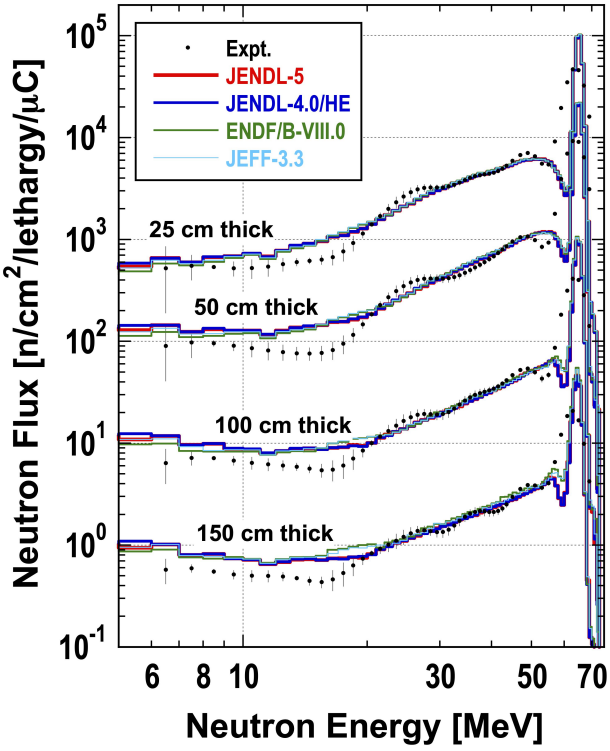

Figure 43. Neutron spectra in TIARA concrete experiment with 65 MeV neutrons.

JENDL-5 are almost the same as those with JENDL-4.0/HE in the whole energy region because the data above 20 MeV of JENDL-5 for materials in concrete are not so modified from those of JENDL-4.0/HE, and show a good agreement with the measured ones. It is noted that the calculated neutron fluxes with ENDF/B-VIII.0 and JEFF-3.3 overestimate the measured ones more with increasing the concrete thickness. This is mainly due to the ^{16}O data, which is pointed out in Ref [42].

4.5.4. Concrete experiment with 65 MeV neutrons

Figures 43 and 44 show the measured and calculated neutron spectra and the C/Es of integrated neutron fluxes of 60–70 MeV and 10–60 MeV in the concrete experiment with 65 MeV neutrons, respectively. As with the experiment with 40 MeV neutrons, the calculated neutron fluxes with JENDL-5 are almost the same as those with JENDL-4.0/HE in the whole energy region. On the contrary, the calculated neutron fluxes with ENDF/B-VIII.0 and JEFF-3.3 overestimate the mea-

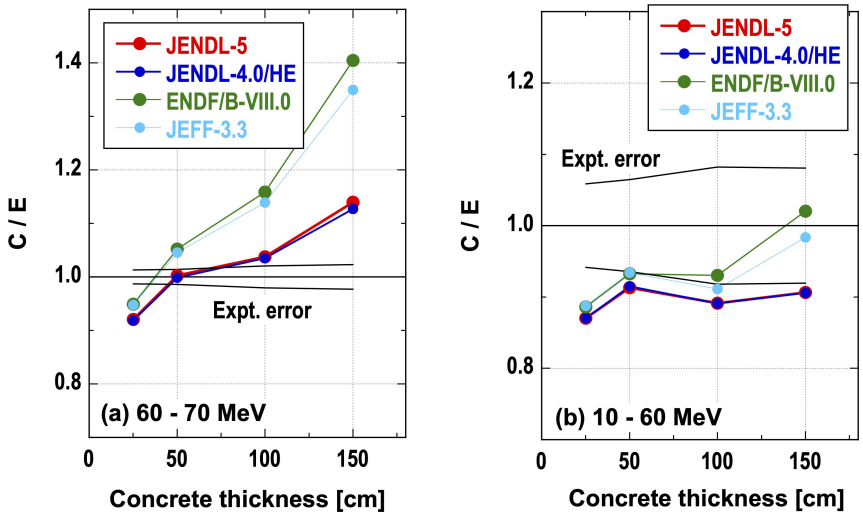

Figure 44. C/Es of integrated neutron fluxes in TIARA concrete experiment with 65 MeV neutrons.

sured data of 60–70 MeV more for the thicker concrete, though those of 10–60 MeV do not.

5. Conclusion

We have validated JENDL-5 released in 2021 under the Shielding Integral Test Working Group in JENDL Committee from the viewpoint of shielding applications with JAEA/FNS in-situ experiments, Osaka Univ./OKTAVIAN TOF experiments, ORNL/JASPER sodium experiments, NIST iron experiment and QST/TIARA experiments. The MCNP code and JENDL-5 were used in the benchmark test. The nuclear data libraries, JENDL-4.0 or JENDL-4.0/HE, ENDF/B-VIII.0 and JEFF-3.3, were also adopted for comparison. The benchmark test results suggest that JENDL-5 improves problems in JENDL-4.0 or JENDL-4.0/HE and provides similar results to or better one than ENDF/B-VIII.0 and JEFF-3.0. The issues improved by JENDL-5 are as follows.

- Neutron fluxes above 10 MeV in FNS in-situ iron experiment
- Neutron fluxes below 1 keV in FNS in-situ iron experiment
- Reaction rates of the ^{197}Au(n,γ)^{198}Au and ^{186}W(n,γ)^{187}W reactions in FNS in-situ copper experiment
- Neutron fluxes below 1 MeV in OKTAVIAN titanium experiment
- Neutron fluxes in OKTAVIAN manganese experiment
- Neutron fluxes above 10 MeV in TIARA iron experiment

We hope that JENDL-5 is used worldwide.

Acknowledgment

The authors acknowledge the JENDL Committee for supporting this study.

ORCID

Seiki Ohnishi http://orcid.org/0000-0002-7358-3767
Naoki Yamano http://orcid.org/0000-0002-3069-1864

References

[1] Iwamoto O, Iwamoto N, Kunieda S. Japanese Evaluated Nuclear Data Library version 5 : JENDL-5. to be published in. J Nucl Sci Technol. DOI:10.1080/00223131.2022.2141903
[2] Kawai M, Hasegawa A, Ueki K. Shielding Benchmark Test of JENDL-3. Japan Atomic Energy Research Institute; 1994. (JAERI 1330).
[3] Shielding Integral Test Working Group (FY2006-2010), Japanese Nuclear Data Committee. Integral Test of JENDL-3.3 Based on Shielding Benchmarks. Japan Atomic Energy Agency; 2019. (JAEA-Research 2018-017).
[4] Shielding Integral Test Working Group, JENDL Committee. JENDL-4.0 Benchmark Test with Shielding Experiments. Japan Atomic Energy Agency; 2021. (JAEA-Research 2021-015).
[5] Tada K, Nagaya Y, Taninaka H, et al. JENDL-5 Benchmark Test for Fission Reactor Applications. Submitted to Journal of Nuclear Science and Technology.
[6] Maekawa F, Yamamoto J, Ichihara C. (Sub Working Group of Fusion Reactor Physics Subcommittee). Collection of experimental data for fusion neutronics benchmark. Japan Atomic Energy Research Institute; 1994. (JAERI-M 94-014).
[7] Ohta M, Takakura K, Ochiai K, et al. Benchmark experiment on titanium with DT neutron at JAEA/FNS. Fusion Eng Design. 2014;89(9–10):2164–2168. DOI:10.1016/j.fusengdes.2014.03.035

[8] Maekawa F, Konno C, Kasugai Y. Data collection of fusion neutronics benchmark experiment conducted at FNS/JAEA. Japan Atomic Energy Research Institute; 1998. (JAERI-Data/Code 98-021).
[9] Kwon S, Sato S, Ohta M, et al. A new integral experiment on copper with DT neutron source at JAEA/FNS. Fusion Eng Des. Available from 2016;109-111: 1658–1662. DOI: 10.1016/j.fusengdes.2015.10.036
[10] Ohta M, Sato S, Kwon S, et al. Integral experiment on molybdenum with DT neutrons at JAEA/FNS. Fusion Engineering Design. 2016;109-111:1644–1648.
[11] Kwon S, Ohta M, Sato S, et al. Lead Benchmark Experiment with DT Neutrons at JAEA/FNS. Fusion Science and Technology. 2017;72: 362–367. DOI: 10.1080/15361055.2017.1330622
[12] Maekawa F, Yamamoto J, Ichihara C. Collection of experimental data for fusion neutronics benchmark. Japan Atomic Energy Research Institute; 1994. (JAERI-M 94-014).
[13] Muckenthaler FJ, Spencer RR, Hunter HT, et al. Measurements for the Jasper Program In-Vessel Fuel Storage Experiment. Oak Ridge National Laboratory; 1992. (ORNL/TM-11989).
[14] Muckenthaler FJ, Spencer RR, Hunter HT. Measurements for the Jasper Program Intermediate Heat Exchanger Experiment. Oak Ridge National Laboratory; 1992. (ORNL/TM-12064).
[15] Stanka MB, Adams JM, Eisenhauer CM. Proton Recoil Measurements of the ^{252}Cf Fission Neutron Leakage Spectrum from an Iron Sphere. Nucl Sci Eng. 2000;134(1):68–76.
[16] Nakashima H, Nakao N, Tanaka S. Experiments on Iron Shield Transmission of Quasi-Mono Energetic Neutrons Generated by 43 and 68 MeV Protons via the ^{7}Li(p,n) Reaction. Japan Atomic Energy Research Institute; 1996. (JAERI-Data/Code 96-005).
[17] Nakao N, Nakashima H, Sakamoto Y. Experimental Data on Concrete Shield Transmission of Quasi-Mono Energetic Neutrons Generated by 43- and 68 MeV Protons via the ^{7}Li(p,n) Reaction. Japan Atomic Energy Research Institute; 1997. (JAERI-Data/Code 97-020).
[18] Yamano N. On the Integral Test Method for Neutron Nuclear Data Evaluation. Ann Nucl Energy. 1997;24 (13):1085–1094.
[19] Bucholz JA. Multidimensional Shielding Analysis of the JASPER In-Vessel Fuel Storage Experiments. Oak Ridge National Laboratory; 1993. (ORNL/TM-12323).
[20] Grundl JA, Spiegel V, Eisenhauer CM et al. A Californium-252 Fission Spectrum Irradiation Facility for Neutron Reaction Rate Measurements. Nucl Technol. 1977;32(3):315–319.
[21] Briesmeister, JF. MCNP -A General Monte Carlo N-Particle Transport Code- Version 4C. Los Alamos National Laboratory; 2000. (LA-13709-M).
[22] Werner, CJ. MCNP User's Manual Code Version 6.2. Los Alamos National Laboratory; 2017. (LA-UR-17-29981).
[23] Shibata K, Iwamoto O, Nakagawa T, et al. JENDL-4.0: a new library for nuclear science and engineering. J Nucl Sci Technol. 2011;48(1):1–30. DOI:10.1080/18811248.2011.9711675.
[24] Kunieda S, Iwamoto O, Iwamoto N. Proceedings of the 2015 Symposium on Nuclear Data. Japan Atomic Energy Agency; 2016. (JAEA-Conf 2016-004).
[25] Brown DA, Chadwick MB, Capote R, et al. ENDF/B-VIII.0: the 8th Major Release of the Nuclear Reaction Data Library with CIELO-project Cross Sections, New Standards and Thermal Scattering Data. Nucl Data Sheets. 2018;148:1–142.
[26] Plompen AJM, Cabellos O, De Saint Jean C, et al. The joint evaluated fission and fusion nuclear data library, JEFF-3.3. Eur Phys J A. 2020;56(181). DOI:10.1140/epja/s10050-020-00141-9
[27] https://rpg.jaea.go.jp/main/en/ACE-J50/ [cited 2022 July 5].
[28] Sato T, Iwamoto Y, Hashimoto S, et al. Features of Particle and Heavy Ion Transport Code System PHITS Version 3.02. J Nucl Sci Technol. 2018;55 (6):684–690. DOI:10.1080/00223131.2017.1419890
[29] https://rpg.jaea.go.jp/main/en/ACE-J40HE/ [cited 2022 July 5].
[30] https://nucleardata.lanl.gov/ace/lib80x/ [cited 2022 July 5].
[31] https://www.oecd-nea.org/dbdata/jeff/jeff33/ cited 2022 July 5].
[32] MacFarlane RE, Kahler AC. Methods for processing ENDF/B-VII with NJOY. Nucl Data Sheets. 2010;111 (12):2739–2890.
[33] Kobayashi K, Iguchi T, Iwasaki S. JENDL Dosimetry File 99 (JENDL/D-99). Japan Atomic Energy Research Institute; 2002. (JAERI 1344).
[34] Konno C, Matsuda N, Kwon S, et al. JENDL-4.0/HE Benchmark Test with Concrete and Iron Shielding Experiments at JAEA/TIARA. EPJ Web of Conference. 2017; 153: 01024. DOI: 10.1051/epjconf/201715301024.
[35] Konno C, Kwon S. Analyses of JAEA/FNS iron in-situ experiment with latest nuclear data libraries. Submitted to EPJ Web of Conference.
[36] Perey FG, Kinney WE, Macklin RL. High resolution inelastic cross section measurements for Na, Si, and Fe. In: Macklin R, editor. Proc. of 3rd Conf. Neutron Cross-Sections and Technology. Vol. 1, Knoxville, TN, USA: National Technical Information Service, U. S. Department of Commerce; 1971. p. 191–195.
[37] Maerten H, Wartena J, Weigmann H. Simultaneous high-resolution measurement of differential elastic and inelastic neutron cross sections on selected light nuclei. 1994. Taken from EXFOR (entry no. 22283).
[38] Kopecky S, Shelley R, Maerten H. High resolution inelastic scattering cross sections in ^{27}Al and ^{23}Na. In: Reffo G, A Ventura, and C Grandi, editors. Proc. Conf. on Nucl. Data for Sci. and Tech. Vol. 1, Trieste, Italy: Italian Physical Society Bologna; 1997. p. 523–525.
[39] Rouki C, Kopecky S, Nankov N, et al. High resolution measurement of neutron inelastic scattering cross-sections for Na-23. Nucl. Instrum. Methods in Physics Res. Sect. A. 2012;672:82–93.
[40] Vanhoy JR, Hicks SF, Chakraborty A, et al. Neutron scattering differential cross sections for ^{23}Na from 1.5 to 4.5 MeV. Nucl Phys Sect A. 2015;939:121–140.
[41] Kinney WE, McConnell JW. High resolution neutron scattering experiments at ORELA. In: Proc. Conf. of Interaction of Neutron with Nuclei, 1976 July 6-9, Lowell, Massachusetts, USA. 1976. Vol.2, p. 1319.
[42] Kwon S, Ohta M, Ochiai K. ENDF/B-VIIIβ4 benchmark test with iron and concrete shielding experiments using 40 and 65 MeV neutrons at QST/TIARA. Fusion Eng Design. 2018;136:2–6.